

RESEARCH

Open Access



Secreted IgM deficiency alters the retinal landscape enhancing neurodegeneration associated with aging

Sarah E. Webster^{1*}, Sydney M. Les^{1,2}, Nico Deleon¹, Daken M. Heck¹, Naomi L. Tsuj¹, Michael J. Clemente^{1,3}, Prentiss Jones⁴ and Nichol E. Holodick^{1,3}

Abstract

Background Maintenance of the retina, part of the central nervous system, and other structures in the eye is critical for vision preservation. Aging increases the prevalence of vision impairment, including glaucoma, macular degeneration, and diabetic retinopathy. The retina is primarily maintained by glial cells; however, recent literature suggests that lymphocytes may play a role in the homeostasis of central nervous system tissues. Natural antibodies are produced by B cells without infection or immunization and maintain tissue homeostasis. Here, we explored the potential role of natural immunoglobulin M (IgM) produced by B lymphocytes in maintaining retinal health during aging in mice.

Results Our results indicate that the vitreous humor of both mice and humans contains IgM and IgG, suggesting that these immunoglobulins may play a role in ocular function. Furthermore, we observed that aged mice lacking secreted IgM (μ s-/-) exhibited pronounced retinal degeneration, accompanied by reactive gliosis, and a proinflammatory cytokine environment. This contrasts with the aged wild-type counterparts, which retain their ability to secrete IgM and maintain a better retinal structure and anti-inflammatory environment. In addition to these findings, the absence of secreted IgM was associated with significant alterations in the retinal pigment epithelium, including disruptions to its morphology and signs of increased stress. This was further observed in changes to the blood-retinal-barrier, which is critical for regulation of retinal homeostasis.

Conclusions These data suggest a previously unrecognized association between a lack of secreted IgM and alterations in the retinal microenvironment, leading to enhanced retinal degeneration during aging. Although the precise mechanism remains unclear, these findings highlight the potential importance of secreted IgM in processes that support retinal health over time. By increasing our understanding of ocular aging, these results show that there is a broader role for the immune system in retinal function and integrity in advanced age, opening new areas for the exploration of immune-related interventions in age-associated retinal conditions.

Keywords IgM, Immunoglobulin, Aging, Retina, Retinal degeneration, Cataracts, Vitreous humor

*Correspondence:

Sarah E. Webster
sarah.webster@wmed.edu

¹Center for Immunobiology, Department of Investigative Medicine, Western Michigan University Homer Stryker M.D. School of Medicine, Kalamazoo, MI 49007, USA

²Department of Medicine, Western Michigan University Homer Stryker M.D. School of Medicine, Kalamazoo, MI 49007, United States of America

³Flow Cytometry and Imaging Core, Department of Investigative Medicine, Western Michigan University Homer Stryker M.D. School of Medicine, Kalamazoo, MI 49007, USA

⁴Department of Pathology, Western Michigan University Homer Stryker M.D. School of Medicine, Kalamazoo, MI 49007, USA



© The Author(s) 2025. **Open Access** This article is licensed under a Creative Commons Attribution-NonCommercial-NoDerivatives 4.0 International License, which permits any non-commercial use, sharing, distribution and reproduction in any medium or format, as long as you give appropriate credit to the original author(s) and the source, provide a link to the Creative Commons licence, and indicate if you modified the licensed material. You do not have permission under this licence to share adapted material derived from this article or parts of it. The images or other third party material in this article are included in the article's Creative Commons licence, unless indicated otherwise in a credit line to the material. If material is not included in the article's Creative Commons licence and your intended use is not permitted by statutory regulation or exceeds the permitted use, you will need to obtain permission directly from the copyright holder. To view a copy of this licence, visit <http://creativecommons.org/licenses/by-nc-nd/4.0/>.

Background

Vision is widely considered one of our most valuable senses. However, the incidence of eye diseases that cause vision loss such as macular degeneration, diabetic retinopathy, and glaucoma rises significantly with age [1]. Therefore, understanding age-related changes in vision is crucial for the development of effective strategies to combat eye diseases and dysfunction. The eye focuses light onto the photosensitive neural tissue at the posterior, the retina, which is an extension of the central nervous system (CNS). The retina contains various types of neurons, including retinal ganglion cells and photoreceptors, which are crucial for initiating and processing visual signals [2, 3].

In response to disease or damage, the retina exhibits diverse reactions and requires stringent balancing of these reactions to resolve damage or disease. Microglia, resident immune cells of the retina, quickly respond to injuries by acting as specialized scavengers and monitoring the retinal environment. When faced with insults such as infection or neuronal damage, microglia become activated, characterized by changes in their morphology and surface markers, and can become either neuroprotective or can contribute to neurotoxicity and inflammation [4–7]. Müller glia and astrocytes, other resident glial cells of the retina, typically respond to injury by undergoing reactive gliosis, which can lead to formation of glial scarring [8]. Despite the retina's immune privilege [9], lymphocytes can enter the retinal tissue under specific conditions, such as during injury, and can exacerbate the inflammatory response of the eye. B lymphocytes in particular play significant roles in various retinal diseases, such as vitreoretinal lymphoma [10], ocular toxoplasmosis [11] and non-infectious uveitis [12, 13].

B cells play a crucial role in fighting bacterial infections through several well-established antibody-mediated mechanisms: (1) neutralizing toxins, (2) opsonizing pathogens, and (3) activating complement, which coats pathogens leading to opsonization and/or lysis [14, 15]. In mice, B cells are categorized into distinct subsets: B2 cells (including follicular and marginal zone B cells) and B-1 cells (comprising CD5+ B-1a and CD5- B-1b cells). Follicular B2 cells initiate a T cell-dependent germinal center response against antigens [16]. Conversely, innate-like B-1 cells produce antibodies independently of T cells and generate natural antibodies [17]. Natural antibodies (NABs) are present in the bloodstream without prior infection or vaccination and serve as an early defense mechanism, allowing time for a specific antibody response to develop [18]. NABs include various isotypes such as IgM, IgA, and IgE, and they play essential roles in: (1) controlling bacterial and viral infections [19–25], (2) aiding in the removal of apoptotic cells and excess autoantigens [26], and (3) binding oxidized low density

lipoprotein (oxLDL), thereby modulating inflammation and preventing atherosclerotic plaque formation [27–30].

B-1 cells are responsible for producing 80–90% of natural antibodies [18], highlighting their significant role in maintaining health and managing disease. Notably, B-1 cells are the predominant B lymphocyte population found in the lacrimal gland of the mouse eye [31]. However, little is currently known about B cells and antibodies within the intraocular compartment of the eye, particularly during healthy aging. Previous studies have shown that the quality of natural antibodies changes during aging, which impacts infection control [32–34].

Herein, we aimed to explore the role of antibodies produced by B cells in the normal physiology of aging eyes. We found that humans and mice had both IgM and IgG in their vitreous humor, which is in contact with the retina. We examined mice lacking secreted IgM ($\mu s^{-/-}$) in old age with regard to retinal health. We found that a lack of IgM leads to significant changes in aging retinas. Enhancing our understanding of how antibodies contribute to maintaining eye health could provide valuable insights for developing advanced therapies that support vision as individuals age. This knowledge may lead to the development of targeted treatments that mitigate age-related vision problems, ultimately improving the quality of life of the aging population.

Methods

Mice

B6;129S4-*Ighm*^{tm1Che}/J mice (referred to as “ $\mu s^{-/-}$ ” hereafter) are unable to produce the secreted form of IgM. The knock-out mice, originally created by Dr. Jianzhu Chen were kindly provided by Dr. Kishore Alugupalli. We backcrossed this line onto a pure C57BL/6J background within our facility and then bred and housed wild type (WT) and homozygous knockouts. Genome scanning was performed to confirm the percentage of C57BL/6J background after backcrossing and was shown to be greater than 94%. Both male and female mice were used at 3–4 months (young) or 18–26 months of age (aged). Mice were housed at five mice per cage on cob bedding with a 12-h light/12-h dark cycle and ad libitum access to water and food. Mice were cared for and handled in accordance with the *Guide for the Care and Use of Laboratory Animals* (National Institutes of Health) and institutional guidelines. All animal studies were approved by the Institutional Animal Care and Use Committee.

Tissue preparations

Enucleations were performed on all euthanized mice. Retinal tissue was isolated as previously published [35, 36]. Briefly, mice were euthanized by CO₂ asphyxiation followed by bilateral pneumothorax. Both eyes were removed, dipped in 70% alcohol and the cornea and lens

Table 1 Antibodies used for Microglia Analysis

Marker	Clone ID	Source	Color
CD11b	M1/70	eBioscience	BB700
CD45	30-F11	BD	APC
CD86	GL1	BD	PE
CD206	C068C2	Biolegend	FITC

were carefully removed from the eye to create an eyecup. The retina was then removed; for most experimentation, the neural retinas were excised first, and the RPE was isolated as well by carefully dissecting it from the choroid via forceps as previously published [37]. For some experimentation, only the lens was removed to maintain eyecups for histology. The excised eyecups or neural retinas were prepared as flat mounts and sectioned or were dissociated to single cell suspensions to be used for flow cytometry, IHC and H&E, or RT-qPCR. In addition, whole eyes were enucleated and fixed in 4% PFA for 15 min before a small window was cut in both the anterior and posterior chambers as per Pang et al., 2021 [38]. Whole eyes were then left in 4% PFA overnight at 4 °C. Lenses were immediately imaged for white-light images post dissection in PBS.

Retinal single cell suspensions

Excised neural retinas were dissociated to a single cell suspension using a modification of the protocol published by Weber et al. (2014) to maintain lymphocyte and microglia cells [39] as traditional methods of retinal dissociations via papain have effects on B cells [40–43]. Briefly, the retinal tissue was subjected to enzymatic digestion with 450 U/mL collagenase I, 125 U/mL collagenase XI, 60 U/mL DNase I, and 60 U/mL hyaluronidase (Sigma) for 1 h at 37 °C with shaking. The neural retina suspension was then passed through a 70 µm filter.

Microglia analysis via flow cytometry

The neural retina cell suspension was filtered through a 70 µm filter and then washed with HBSS + 10% FBS solution. Cells were spun down and supernatant was removed. Cells were then resuspended in the HBSS wash solution and stained with Fc block for 15 min followed by staining with the following antibodies (1:1000) for 15 min on ice in the dark as previously described [4] (Table 1):

The labeled cells were run on a BD FortessaSORP (BD Biosciences). Images were constructed with FlowJo 10.10

software (BD Biosciences). The presence of various auto-fluorescent cells in the retinal single cell suspensions necessitated specific fluorochrome combinations to avoid highly auto-fluorescent channels. In addition, use of fluorescence minus one (FMO) controls were essential in guiding gating strategies.

Immunohistochemistry and H&E staining

For immunohistochemistry, antibody labeling was performed as previously described [35]. Briefly, after fixation, tissue was permeabilized, post-fixed, and then stained with 1° antibodies diluted in BlockAid (1% v/v; ThermoFisher). Antibody staining was carried out using the antibodies listed in Table 2. Primary antibodies were detected with secondary antibodies (3.33 µl/mL) per Table 2. Nuclei were counterstained with DAPI (0.1 µg/mL; Sigma) or Sytox Green (5 mM; ThermoFisher). Retinas were prepared either as flat mounts or sections (gelatin embedded; cut at 15 µm) and mounted in Prolong Gold (Thermo).

For H&E staining, either whole eyes or eye cups were used. Whole eyes were cyrosectioned (18 µm) before mounting on slides. RPE flat mounts were adhered to slides post-fixation. H&E protocol was performed as per Pang et al., 2021 with the slides being processed in staining jars before mounting [38]. For F-actin staining, RPE flat mounts were stained with Phalloidin Alexa-Fluor 488 (Thermofisher).

Lens analysis

Mouse lenses were dissected immediately from freshly enucleated eyeballs in 1X Dulbecco's phosphate buffered saline (DPBS). Images of freshly dissected lenses were captured using an Stereomaster Dissection Scope (Fisher) with a digital Nikon camera. Axial diameter (top to bottom) and equatorial diameter (left to right) for each lens was measured to calculate lens volume with the following equation, where r_E is the equatorial radius and r_A is the axial radius:

$$volume = \frac{4}{3} \times \pi \times r_E^2 \times r_A$$

Vitreous humor analysis of total IgM and IgG

Murine vitreous humor was collected from eyes after enucleation, modified from previous methodology [44].

Table 2 Primary and secondary antibodies used

Primary Antibody	Dilution	Source	Secondary Antibody	Source
Goat anti-Iba-1	7.5 µl/mL	Abcam; ab98887	Donkey anti-goat AF405 or AF 488	Abcam; ab175700
Chicken anti-GFAP	3.4 µl/mL	Abcam; ab4674	Donkey anti-chicken AF647	Jackson; #703-605-155
Rabbit anti-IL-1β	10 µl/mL	Abcam; ab205924	Donkey anti-rabbit AF488 or AF568	Abcam; ab150073
Rabbit anti-Caspase-3	3.4 µl/mL	Abcam; ab44976	Donkey anti-rabbit AF488 or AF568	Abcam; ab150073
Rabbit anti-Thy1.2/CD90	3.4 µl/mL	Abcam; ab273071	Donkey anti-rabbit AF488 or AF568	Abcam; ab150073

Briefly, under a dissection scope, enucleated eyes were pierced intravitreally with an insulin syringe backfilled with 100 μ L sterile PBS which was used to aspirate vitreous humor. Using this method around 5–10 μ L of vitreous humor was able to be collected from each eye. The murine vitreous humor was frozen post collection, thawed, and then was analyzed for total IgM or IgG by ELISA according to the manufacturer's instructions (Bethyl Laboratories). For human vitreous humor collections, trained medical examiner personnel collected vitreous specimens from deceased individuals ($n = 10$ males; $n = 10$ females; aged 18–32) as part of routine autopsy procedures. Using a 10-cc syringe with a 18-gauge needle attached, the side of the eye was approached with the bevel of the needle facing upward and the needle positioned at a 70–80° angle. The globe of the eye was punctured while slowly advancing the needle. Typically, the needle tip can be seen through the pupil, and this served as a guide to prevent advancing the needle through the posterior aspect of the eye. While holding the syringe steady, the syringe plunger was drawn backwards. The collected vitreous sample was transferred into a tube that contained a clot activator but no preservatives, separating material, or anticoagulants. The tube was gently inverted 8–10 times then stored at -20 °C until analysis. Human vitreous humor samples were thawed on ice and then analyzed for total IgM or IgG by ELISA. Both murine and human ELISAs were performed according to the manufacturer's instructions (Bethyl Laboratories). Analyses were done using GraphPad Prism (v10.2.1).

RT-qPCR

For gene expression analysis, RNA was isolated from retina or RPE/choroid tissue using the Direct-zol RNA Miniprep Kit (Zymo) following the protocol provided. RNA was quantified using the Qubit 3 and the quality of RNA was verified using the RNA pico kit for a Bioanalyzer (Aligent). RNA with a RIN > 8 was used for all reactions. PrimeTime Assays (IDT TaqMan chemistry) were used for the genes listed in Table 3. Efficiencies of all assays were determined to be between 90 and 110%. Assays were run using the SuperScript III Platinum

One-Step Kit for qRT-PCR with ROX (ThermoFisher). 10 ng of RNA was used for each reaction in 20 μ L reactions per the manufacturers protocol. Each sample was run in triplicate. For each group, $n > 5$ retinas were pooled, and reactions were run with the following cycling parameters: a 50 °C hold for 15 min for cDNA synthesis followed by a 95 °C for 2 min polymerase activation. This was followed by 40 cycles of 95 °C for 15 s and annealing/extension at 60 °C for 30 s on the Quantstudio 3. The endogenous reference genes ActB and B2M were averaged to be used as internal references to calculate the relative gene expression for each group, as previously published [33]. The $2^{-\Delta C_t}$ method was used to calculate relative gene expression for each group compared to the housekeeping genes.

Imaging & cell counts

All flat mounts and sections were imaged using a Nikon A1R+scanning laser confocal microscope (Nikon) or Nikon Eclipse Ts2 microscope (Nikon). For RPE nuclear counts, Iba-1+ cell counts, and caspase-3+ cell counts, cells were counted from four quadrants in 200 μ m² sections and averaged to represent an "n" of 1 as previously described [35, 36]. The counts from these four quadrants were averaged to account for eccentricities in cell numbers across the retina and RPE. Normalization was required in these studies due to variations in retinal counts obtained in each section due to the normal variations found between the location (central to peripheral) of the section. All experiments were repeated in $n > 5$ mice/group (specific n values are listed on each figure legend) and counts were normalized to the total number of cells in each image. Quantitative analysis was done using ImageJ software (NIH).

For measuring the width of the ONL and INL three different areas of a section were measured and averaged from 10 sections per retina in each of the four quadrants; each quadrant was averaged for the datapoint for $n > 5$ animals per group. We analyzed microglia morphological changes by determining the transformation index (TI) of microglia as described [45, 46]. To measure TI, 40X images were converted to 32-bit in ImageJ analysis software and individual microglia cells were traced to determine the perimeter and area of a microglia cell. TI was calculated using the equation:

$$TI = \frac{\text{perimeter}^2}{4\pi \times \text{area}^2}$$

The TI was calculated for 5–7 microglia per 40X image, looking at all areas of the retina (central, medial, and peripheral) for a minimum of 50 quantified microglia per animal with a minimum of 8–10 animals in each age and sex group. Values are expressed as a range of 1 to 100, with a TI value of 1 representing a circular, amoeboid

Table 3 IDT PrimeTime assays used

Gene ID	Assay ID
IL-1 β	Mm.PT.58.41616450
CXCL13	Mm.PT.58.31389616
IL-10	Mm.PT.58.13531087
TNF α	Mm.PT.58.12575861
VEGF	Mm.PT.58.31754187
IL-13	Mm.PT.58.31366752
IL-6	Mm.PT.58.10005566
ActB	Mm.PT.58.22214843.g
B2M	Mm.PT.39a.22,214,835

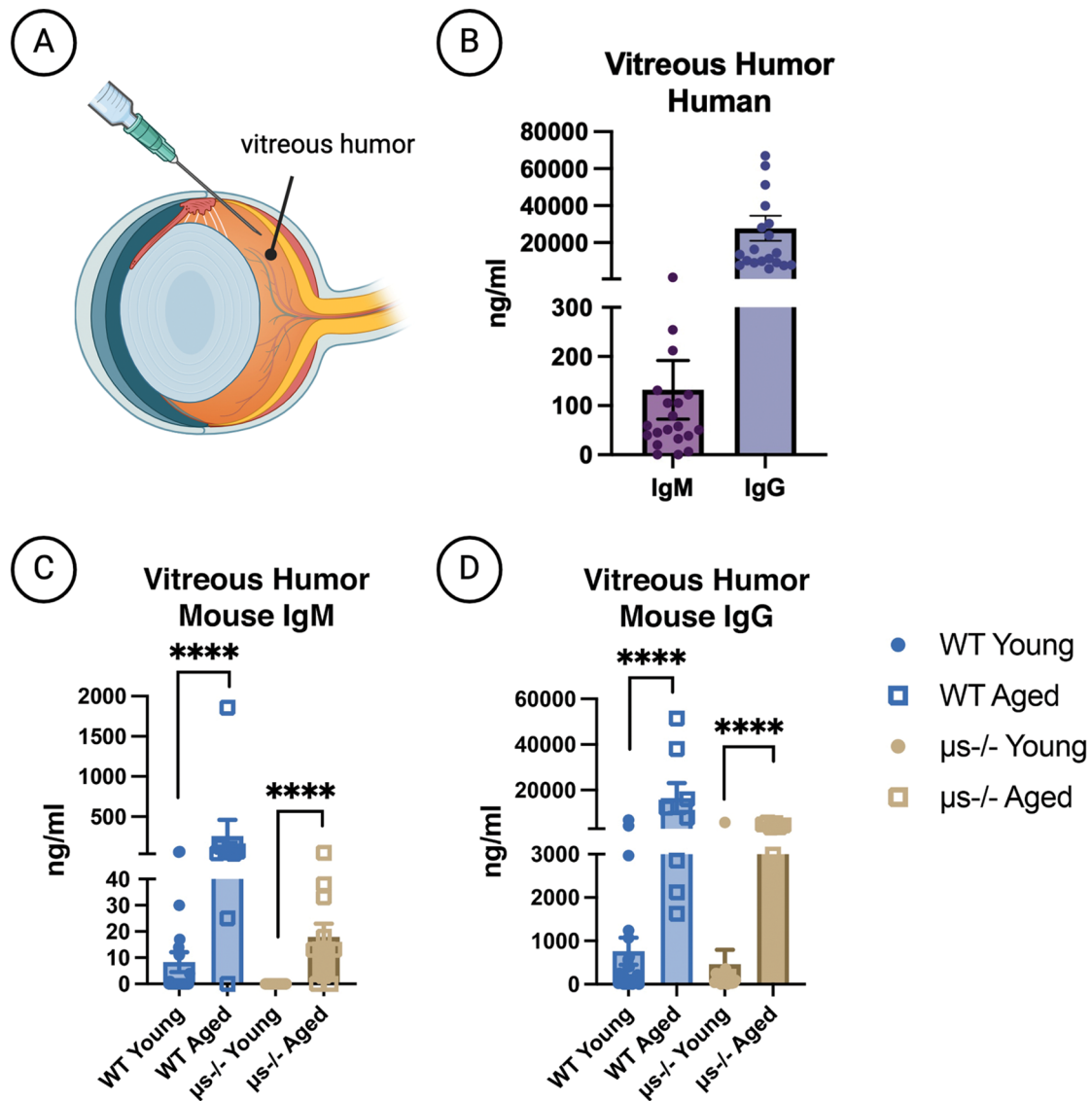


Fig. 1 Immunoglobulin is found in the vitreous humor of mice and humans. **(A)** Schematic showing sampling of vitreous humor from the mouse eye. **(B)** Vitreous humor collected from human donors ($n=20$) were frozen at -80°C , thawed on ice, and then evaluated for IgM and IgG using ELISAs. **(C-D)** Vitreous humor was collected from both male and female young WT ($n=25$), aged WT ($n=9$), young μ s-/- ($n=17$), aged μ s-/- ($n=11$) mice. The murine vitreous humor was frozen at -20°C , thawed on ice, and then evaluated for IgM **(C)** and IgG **(D)** using ELISA. Samples run were averaged across five independent experiments. Statistics used: Mann-Whitney test; **** $p < 0.0001$. Created in BioRender. Webster, S. (2023) BioRender.com/x81m962

activated microglia cell with fewer/shorter cellular processes while higher TI values represent ramified microglia cells with extensive branching and smaller cell bodies. All image counts were performed blindly by two independent investigators.

To quantify the percent immunoreactive area of GFAP+glia, raw confocal images were converted into 32-bit in ImageJ analysis software (NIH) and an automatic threshold was applied. Data was normalized by volume based on XYZ coordinates to account for changes in z-stack thickness and image size. For GFAP+astrocytes, individual astrocyte cell body intensity was measured, and the averaged total intensity was plotted using ImageJ.

Human cytokine measures from blood serum

The analysis was performed using Biochip Array Technology (BAT). BAT incorporates the use of a solid-state platform which has discreet test regions that are coated with immobilized antibodies specific to different biomarkers of cytokines and growth factors. A sandwich chemiluminescent immunoassay was employed for the array. Elevated levels of the cytokine biomarkers in a specimen result in an increase in binding to antibody labelled with horseradish peroxidase and thus an increase in the chemiluminescent signal emitted.

Statistics

Statistical analyses were performed using Prism (v10.2.1). All statistical analyses used are indicated in each figure legend. All analyses were reported with mean \pm SEM with $p < 0.05$ being considered statistically different. A biostatistician was consulted for appropriate statistical measures.

Results

Immunoglobulin is present in the vitreous humor of mice and humans

In the late 1970s, two independent reports in humans demonstrated the presence of immunoglobulins (Ig) in the aqueous humor of the eye [47, 48], suggesting that there might be potential immunological role in the ocular compartment despite its immune privilege. Further, in the 1990s, a report showed that small amounts of Ig were detected in the vitreous humor (VH) of humans with retinal detachment [49], indicating that changes in Ig levels might be associated with retinal pathology. Given the well-established role of Ig in immune regulation and tissue homeostasis, we hypothesized that Ig, particularly IgM, might also be present in the vitreous humor under normal physiological conditions and during aging. Furthermore, as aging is a significant risk factor for retinal degeneration, we sought to determine whether secreted IgM contributes to maintaining retinal health and modulating inflammation in the aging eye.

Here, we collected VH from euthanized mice (Fig. 1A) and deceased humans (Fig. 1B). We found both IgM (74.31 ng/mL \pm 15.69 SEM) and IgG (19951.0 ng/mL \pm 3847 SEM) in human VH from males and females (Fig. 1B). Furthering these findings, we examined VH obtained from the eyes of wild-type (WT) mice and found both IgM (31.6 ng/ml \pm 5.6 SEM) and IgG (761.0 ng/ml \pm 312.1 SEM) (Fig. 1C and D). Furthermore, in aged WT mice we observed a significant increase in the amount of IgM (390.0 ng/ml \pm 200.3 SEM) and IgG (16507.0 ng/ml \pm 6528.0 SEM) as compared to young WT mice (Fig. 1C and D). We also examined mice lacking the ability to secrete IgM, secretory IgM knockout mice (μ s^{-/-}); however, these mice can generate surface IgM and secrete all other antibody isotype classes. We observed a significant increase in the amount of IgG in aged μ s^{-/-} mice (3210.0 ng/ml \pm 592.1 SEM) as compared to young μ s^{-/-} mice (459.4 ng/ml \pm 332.9 SEM) (Fig. 1D). Surprisingly, we also saw a significant increase in the amount of VH IgM in aged μ s^{-/-} mice (43.27 ng/ml \pm 7.76 SEM) as compared to young μ s^{-/-} mice (1.88 ng/ml \pm 1.31 SEM) (Fig. 1C). Secreted IgM should be completely absent in μ s^{-/-} mice, as observed in the serum of these mice (Supplementary Figure S1). However, the amount of IgM observed in the VH of aged μ s^{-/-} mice was significantly

lower than that observed in aged WT mice (43.27 ng/ml vs. 459.4 ng/ml) (Fig. 1).

Together, these results demonstrate a significant amount of IgM and IgG within the VH of both humans and mice. Additionally, we found that VH Ig levels in WT mice increased with age. However, little is known about how Ig might enter the vitreous humor, particularly considering the presence of IgM in the vitreous humor of μ s^{-/-} mice, which have B cells that are unable to secrete IgM.

Lack of secreted IgM enhances age-related retinal degeneration

After identifying age-related changes in IgM and IgG levels in the vitreous humor, we explored whether IgM is involved in the process of maintaining retinal health during aging. We observed significant changes in the retinal structure of aged μ s^{-/-} mice compared to aged WT mice (Fig. 2A). Retinal thickness is known to decrease with age, and retinal thinning is associated with CNS degeneration [50, 51]. When we measured total retinal thickness, the lack of IgM led to a significant reduction (246.7 μ m \pm 2.216 SEM aged WT to 205.2 μ m \pm 1.195 SEM aged μ s^{-/-}; Fig. 2B). Each individual neural layer (ONL, INL, and GCL) was measured. The ONL, primarily composed of photoreceptor cell bodies, was significantly decreased with lack of IgM (69.71 μ m \pm 3.4 SEM vs. 55.5 μ m \pm 0.98 SEM; Fig. 2C). Similarly, the INL, which houses several types of retinal neuron cell bodies, was decreased in the mouse model lacking secreted IgM (Figs. 2D and 46.25 μ m \pm 1.31 SEM vs. 29.26 μ m \pm 1.52 SEM). The GCL is composed of retinal ganglion cell bodies and their axons, which constitute the optic nerve. We also counted the GCL from Thy1.2⁺ retinal ganglion cells (Fig. 2E and F). When we quantified these flat mounts, we found that the total cell count decreased from aged WT (48.33 cells/ μ m² \pm 1.66 SEM) to aged μ s^{-/-} (40.83 cells/ μ m² \pm 0.61 SEM) (Fig. 2E). Taken together, these data indicate that the lack of secreted IgM from B cells leads to enhanced age-related neurodegeneration across different retinal cell layers.

IgM plays many roles in maintaining physiological functions in addition to its ability to protect against infections. The essential role of IgM for the clearance of apoptotic cells has been well established [26, 52–54]. As the loss of cell density was enhanced in aged μ s^{-/-} mice, we next asked whether density loss was associated with cell death occurring in aged μ s^{-/-} mice. Examination of caspase-3 expression in aged WT and μ s^{-/-} mice (Fig. 3) revealed apoptotic cells (*caspase-3*⁺) were found largely in μ s^{-/-} mice only (Fig. 3A vs. B). Aged WT mice had 1.67 \pm 0.45 *caspase-3*⁺ cells per retinal section (SEM), but loss of secreted IgM (aged μ s^{-/-}) drastically increased the number of apoptotic cells to 20.83 \pm 0.824 *caspase-3*⁺ cells

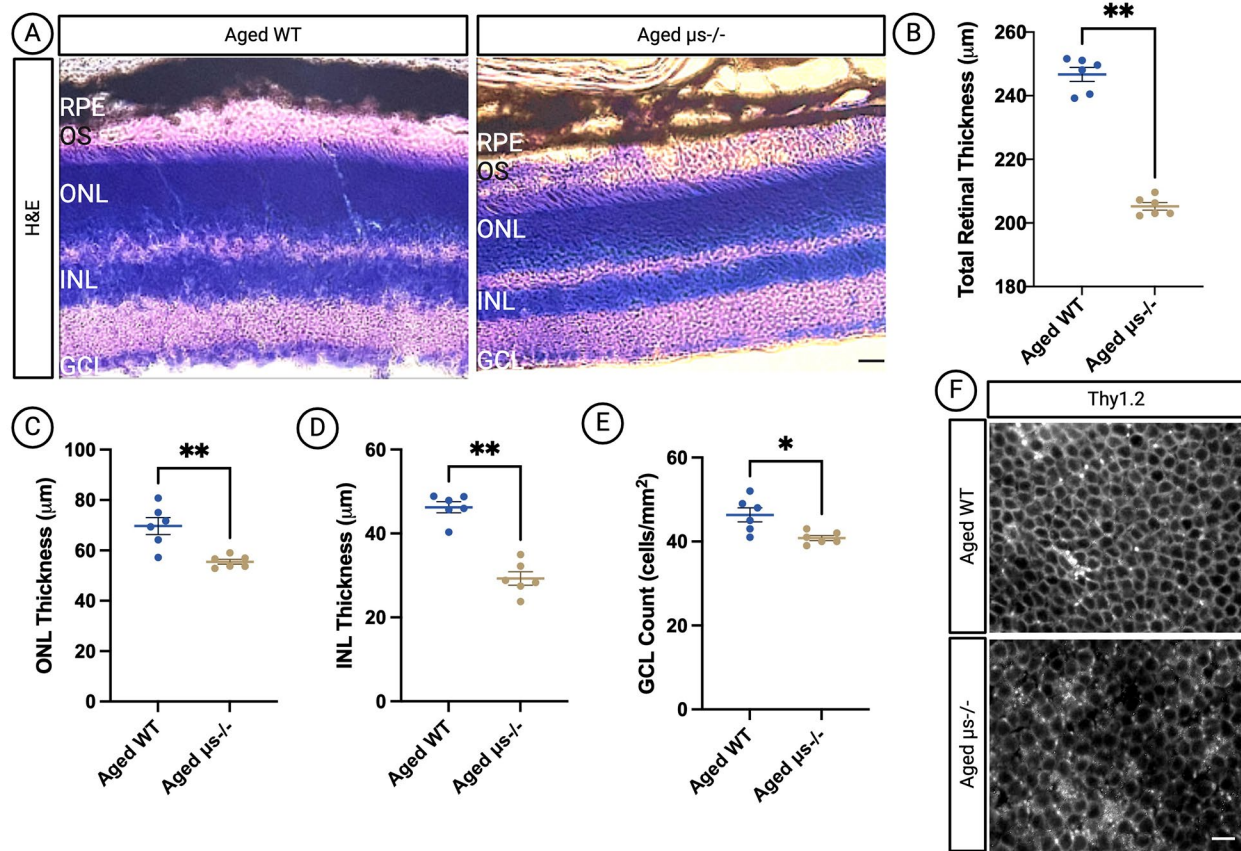


Fig. 2 Lack of secreted IgM leads to enhanced age-related retinal degeneration. **(A)** Retinas from aged WT and $\mu s^{-/-}$ mice were fixed, sectioned, and then underwent H&E; RPE: retinal pigment epithelium, OS: outer segments, ONL: outer nuclear layer, INL: inner nuclear layer, GCL: ganglion cell layer. **(B)** Total retina thickness was quantified from OS to GCL. **(C)** ONL thickness, **(D)** INL thickness, and **(E)** GCL cell count were all measured as presented in material and methods. **(F)** Retinas from aged WT and $\mu s^{-/-}$ were fixed, sectioned, and then underwent IHC for Thy1.2 (RGC marker) to visualize loss of GCL density as measured in **(E)**. Results are based on two independent experiments with each data point representing the final average for each measurement for one animal as described in the materials and methods. Aged WT: $n=6$. Aged $\mu s^{-/-}$: $n=6$. Statistics used: Mann-Whitney. * $p < 0.05$, ** $p < 0.01$. Scale bar = 50 μm

per section (SEM) (Fig. 3E; $p < 0.0001$). Additionally, we examined apoptosis using TUNEL staining. We found that aged WT mice (Fig. 3C and F) had on average 1.2 ± 0.03 (SEM) TUNEL-positive cells per retinal section, while aged $\mu s^{-/-}$ mice (Fig. 3D, F) had 4.3 ± 0.1 (SEM) ($p < 0.0001$). Together, these data suggest that the loss of retinal density in aging mice lacking secreted IgM is apoptotic-based cell death. Since mice homozygous for the *rd8* allele exhibit retinal degeneration, we verified that the $\mu s^{-/-}$ and WT mice are on the C56BL/6J background, and do not carry the *rd8* mutant allele found in mice on the C56BL/6 N background [55, 56] (Fig. 3G).

Significant changes in the inflammatory profile of the retina in the absence of secreted IgM

Natural IgM has been reported to play a role in restraining the development of inflammation by clearing apoptotic cells [57, 58]. With the large amount of apoptosis seen in $\mu s^{-/-}$ mice (Fig. 3), we hypothesized that retinal inflammation would be increased compared to that in

WT mice. RT-qPCR analysis of RNA isolated from neural retinas revealed a significant increase in the levels of pro-inflammatory cytokines IL-6 (Fig. 4A), IL-1 β (Fig. 4B), TNF α (Fig. 4C), and VEGF (Fig. 4D) from $\mu s^{-/-}$ retinas as compared to WT retinas, and this significant increase was enhanced with aging. In both young and aged WT mice, pro-inflammatory cytokine expression remained very low (Fig. 4A-D, blue bars). IL-6 plays an important role in ocular inflammation [59], and we observed no change in IL-6 expression in aged WT retinas compared with young retinas (Fig. 4A). However, in the absence of IgM, IL-6 levels significantly increased in aged $\mu s^{-/-}$ retinas. Other pro-inflammatory cytokines involved in ocular inflammation, including IL-1 β , TNF α , and VEGF, all displayed low-levels of expression during aging in WT retinas, but in both young and aged $\mu s^{-/-}$, these cytokine levels were significantly higher than those in WT retinas (Fig. 4B-D).

Anti-inflammatory cytokines, including IL-13 and IL-10, are important for the suppression of ocular

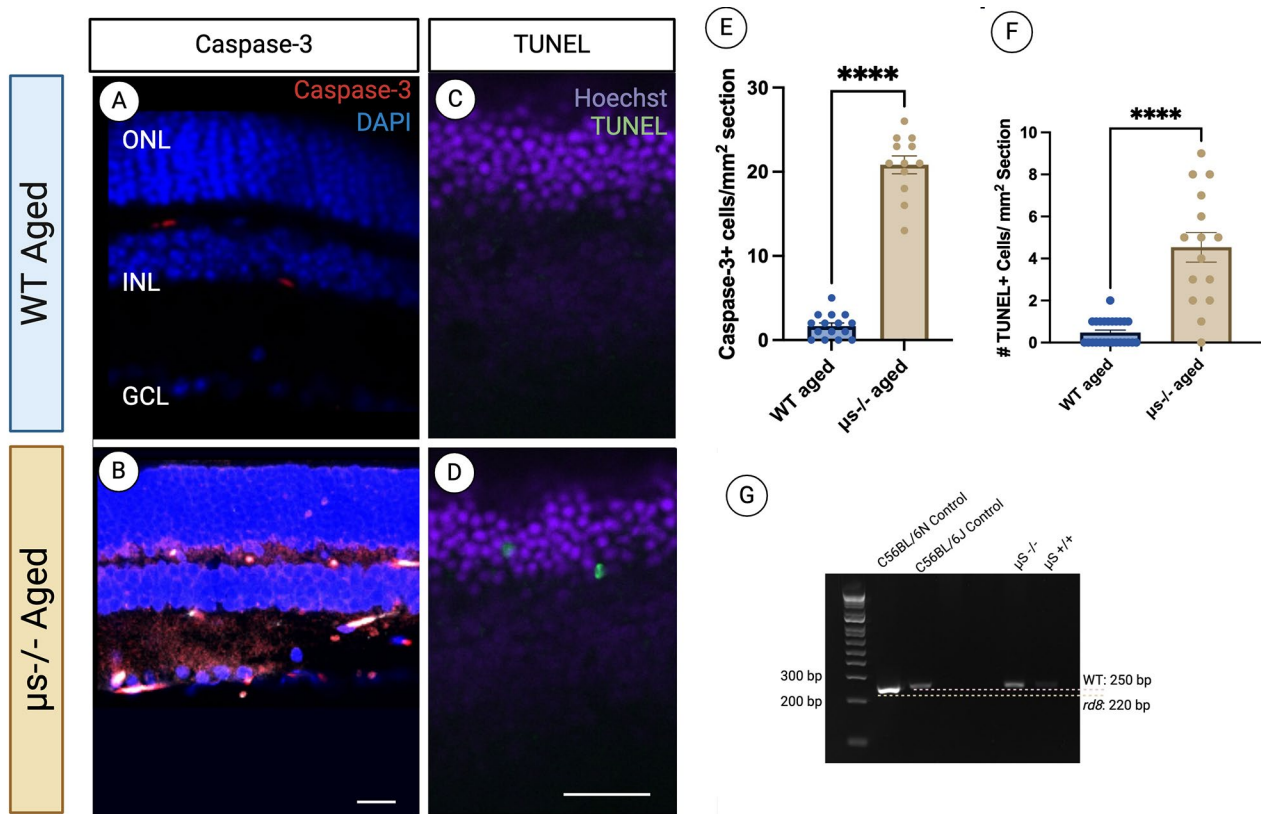


Fig. 3 Retinal degeneration with lack of IgM is due to cellular death. Aged WT and $\mu s^{-/-}$ retinas were evaluated for presence of cellular death using detection of (A & B) caspase-3 (red) and (C & D) TUNEL (green). Quantification of caspase-3-positive cells (E) and TUNEL-positive cells (F). Results are based on two independent experiments with each data point representing total number of positive cells per section, with 5 sections measured for each animal. Aged WT: $n=5$. Aged $\mu s^{-/-}$: $n=3$. Statistics used: Mann-Whitney. **** $p < 0.0001$. Scale bar = 50 μm . (G) Endpoint PCR was run from DNA extracted from ear punches on both WT ($\mu s^{+/+}$) and KO ($\mu s^{-/-}$) mice on the μs background. B6/N and B6/J sourced from Jackson were used as a positive and negative control. Results based on five independent experiments with $n=10$ mice per each group.

inflammation and play an important role in CNS homeostasis by limiting the damaging effects of neuroinflammation [60]. Probing the expression of IL-10 and IL-13 in the retina, we found that levels of IL-13 were increased significantly in aged WT mice (Fig. 4E). Interestingly, in $\mu s^{-/-}$ mice, IL-13 levels were significantly decreased to barely detectable levels. Similarly, IL-10 expression (Fig. 4F) was maintained into old age in WT mice but was significantly decreased in young $\mu s^{-/-}$ mice compared to their WT counterparts. The aged $\mu s^{-/-}$ retinas showed almost non-existent IL-10 levels (Fig. 4F). Interestingly, the pro-inflammatory chemokine CXCL13, which is produced largely by microglia in the retina [61, 62], is also increased specifically in the aged $\mu s^{-/-}$ population alone (Fig. 4G). Together, these data highlight an important role for IgM in the neural retina in maintaining a cytokine environment that promotes anti-neuroinflammatory states and suppresses pro-inflammatory cytokines during aging.

We further examined cytokine profiles in human serum from young and old individuals to explore parallels with our mouse model findings. Similar to the mouse data,

we observed an increase in the pro-inflammatory cytokine VEGF with age in humans (Supplemental Figure S2). However, unlike the dramatic inflammatory shift associated with the absence of IgM in mice, age alone did not lead to significant changes in the overall inflammatory profile in human serum. While serum provides insights into systemic inflammatory changes, it may not fully capture localized inflammatory processes within the eye.

Since lack of IgM led to a complete reversal of the inflammatory cytokine profile in the $\mu s^{-/-}$ retinas compared to WT retinas, we hypothesized that the resident microglia would also be affected by the absence of secreted IgM and subsequent changes in cytokine levels, as microglia cells are the resident immune cells of the CNS [63]. We first determined whether there were changes in microglia numbers within the WT and $\mu s^{-/-}$ mice by quantifying the number of Iba-1+ cells within the retinas of each group using IHC. It is important to note that Iba-1 can also label macrophages, which can expand in aging CNS tissue [64, 65]. We found that the total number of Iba-1+ microglia increased significantly with old age, regardless of the presence of IgM

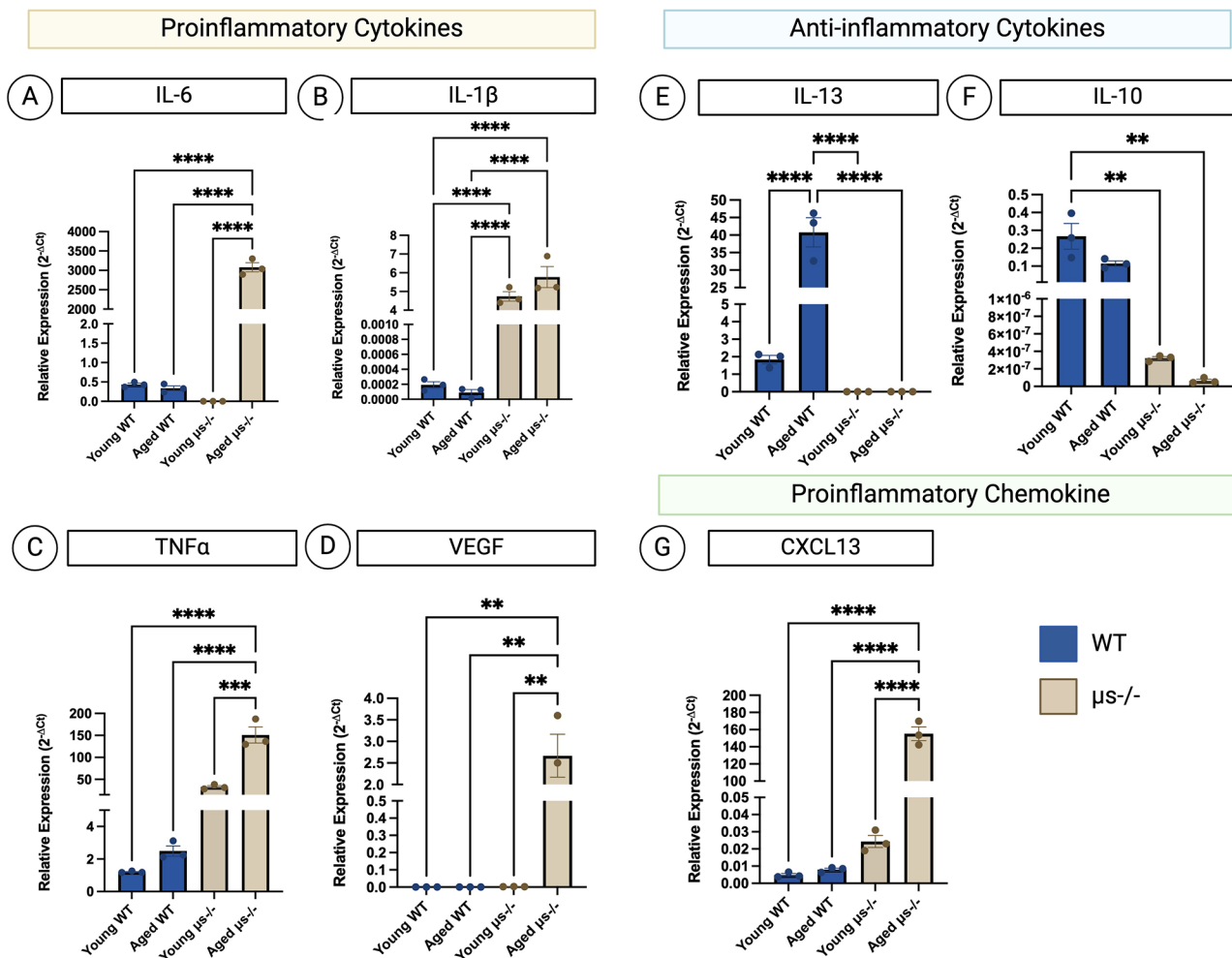


Fig. 4 IgM plays an important role in maintenance of retinal anti-inflammatory cytokines during aging. Neural retinas were isolated from young (3-4mo) or aged (24-26mo) WT and KO eyes. RNA was isolated from the retinas and qPCR was done to determine levels of proinflammatory cytokines (A-D), anti-inflammatory cytokines (E-F), and proinflammatory chemokines (G). Gene expression ($2^{-\Delta C_t}$) was calculated for each gene run in triplicate from the average of three independent experiments, and then plotted for each group. Animal numbers: $n=6$ retinas per group. Statistics used: ANOVA with Kruskal Wallis post-hoc analysis. * $p < 0.05$, ** $p < 0.01$, *** $p < 0.001$

(Supplementary Figure S3), consistent with previous literature [5, 9]. We then assessed morphological changes of the resident microglia by measuring the transformation index (TI) of the microglia (Supplementary Figure S3). Microglia retained higher TI values with a ramified morphology and small cell bodies in the young mice as compared to the aged mice. The TI index significantly decreased in young μs^{-/-} mice compared to young WT mice ($p=0.028$; Welch's test), indicative of microglia with a more amoeboid morphology with retracted cellular processes and larger cell body. Interestingly, aging dramatically decreased the TI value of microglia compared to young groups (WT: $p=0.0051$; μs^{-/-}: $p=0.0166$; Welch's test). These data indicate that aging results in increased microglia in the retina and a significant change in microglia morphology.

With the significant changes in retinal cytokine profiles and changes in microglia numbers as well as morphology, we hypothesized that microglia in the μs^{-/-} mice might be differentially polarized; CD86⁺ microglia have been shown to release pro-inflammatory factors whereas CD206⁺ microglia secrete anti-inflammatory factors [5]. However, it is worth noting that using CD86 and CD206 alone to discuss polarization states may be simplified in light of recent literature [66] and as such, further characterization and functional assays are necessary to determine the full activation state of these microglia. To examine the polarization phenotype of activated microglia in μs^{-/-} mice, flow cytometry was performed on whole-neural retina single-cell suspensions from both young and aged WT and μs^{-/-} mice (Fig. 5A-B; Supplementary Fig. S4). As seen with IHC, total microglia (CD45⁺CD11b⁺) increased in aged mice, regardless of

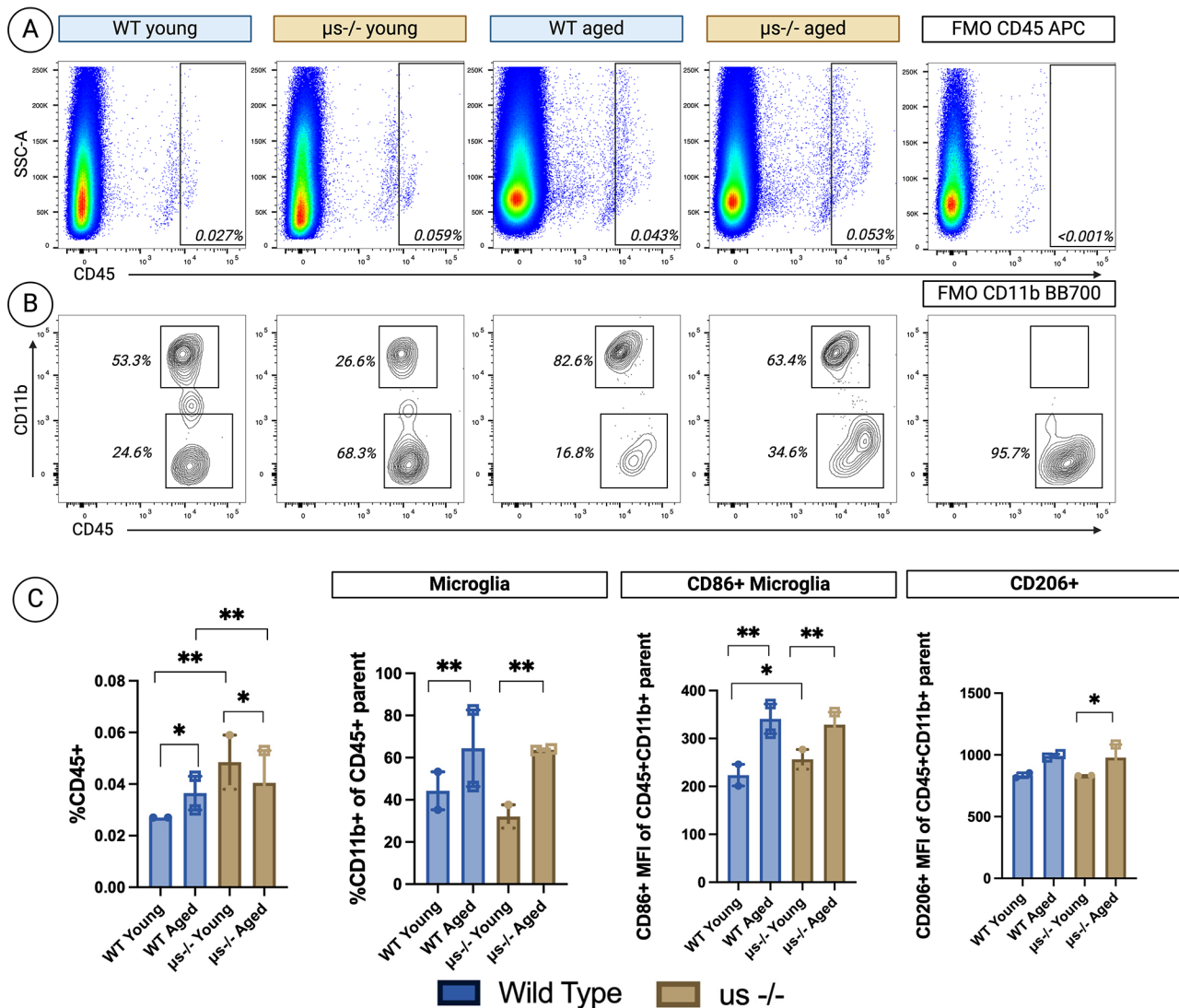


Fig. 5 Microglia are increased in the aged retina. Young (3–4mo) and aged (18–26mo) WT and $\mu s^{-/-}$ neural retinas were isolated and processed to a single cell suspension. **(A)** Representative FACS plots show gating on CD45+ cells. The average percent of retinal CD45+ cells is shown. **(B)** Representative FACS plots show gating for CD45+CD11b+ microglia. **(C)** Graphs showing the total percent of CD45+ cells found in retinal cell preps, the percent of CD45+CD11b+ microglia, and median fluorescent intensity (MFI) of CD86 and CD206. FMO, fluorescence minus one. Total Retinas: young WT $n = 12$; Aged WT $n = 28$; young $\mu s^{-/-}$ $n = 12$; aged $\mu s^{-/-}$ $n = 26$. Results based on two independent experiments with retinas from individual mice pooled in each of the two experiments. Statistics: ANOVA with Kruskal Wallis post-hoc analysis; * $p < 0.05$, ** $p < 0.01$, *** $p < 0.001$

the presence or absence of IgM (Fig. 5C). Interestingly, age was the driver of the change in microglia regardless of the presence of secreted IgM (Fig. 5C). In the microglia of young $\mu s^{-/-}$ mice, there was a significant increase in the MFI of CD86 compared to young WT mice ($p = 0.0437$), despite no change/increase in total microglia (CD45+CD11b+) between WT and $\mu s^{-/-}$ retinas ($p = 0.1154$). Together, these data indicate that the absence of secreted IgM leads to an increase in the MFI of CD86 on microglia in young $\mu s^{-/-}$ mice, and with age, regardless of the presence or absence of IgM, there is an increase in the MFI of CD86 on microglia in the retina, which is indicative of activation.

Lack of IgM leads to gliosis in the retina and degradation of retinal barrier integrity

In addition to microglia, the retina contains astrocytes and Müller glia (MG), which preform critical roles in homeostasis. MG span the entire retinal thickness and play essential roles in structural integrity, retinal metabolism, neurotransmitter uptake, retinal homeostasis, and importantly, cytokine production [8]. Astrocytes, which are largely restricted to the nerve fiber layer, have close relationships to blood vessels and neurons and play an important role in the blood-retinal barrier (BRB) as well as in neuronal survival [8]. During neurodegenerative processes, both the MG and astrocytes display activation

and gliosis. A hallmark of gliosis is the upregulation of glial fibrillary acidic protein (GFAP). Gliosis initially has beneficial effects on neuroprotection, but chronic gliosis is associated with retinal swelling and inflammation, BRB breakdown, and neurodegeneration [8]. Since microglia displayed activation and gliosis in aging μ s^{-/-} mice, we next investigated whether there was evidence of reactive gliosis in other glia of these retinas.

First, we examined astrocytes in retinas of WT and μ s^{-/-} mice. No differences were observed in astrocyte density, morphology, or GFAP expression when comparing young mice. However, looking at aged WT and μ s^{-/-} mice (18-26mo) there were significant differences in the astrocyte population within the retina (Supplemental Figure S5). We examined changes in total GFAP expression and GFAP expression within astrocyte cell bodies to determine if lack of IgM was associated with gliosis. GFAP expression, as marked by the total percentage of GFAP reactivity within the nerve fiber layer, was measured from flat-mount images. As evident by the increase in GFAP expression, lack of IgM significantly increased reactive astrocytes in the retina ($11.2\% \pm 2.3$ vs. $14.8\% \pm 1.1$; $p < 0.0001$; Welch's test). Looking at the cell bodies of astrocytes, there was marked thickening of cell body density. We quantified this change in ImageJ by selecting astrocyte cell bodies and examining the average intensity of GFAP staining between the WT and μ s^{-/-} flat mounts (Supplemental Figure S5). We observed a significant shift in GFAP intensity within the cell bodies between WT (blue histogram) and μ s^{-/-} (brown histogram) astrocytes. These data demonstrate that lack of IgM leads to reactive astrocytes within the murine retina with age.

Next, we examined GFAP expression in sections of aged WT and μ s^{-/-} mice. As GFAP stains both astrocytes and MG, we examined both individually based on their morphology and localization within retinal layers. Retinal sections depicting MG are shown, with MG being highlighted based on their morphology (Fig. 6A-B). Gliosis was significantly increased in the absence of IgM in the aged groups (Fig. 6C; $p = 0.0041$), as there were drastic amounts of GFAP in the μ s^{-/-} retinas (Fig. 6B) as compared to the WT group (Fig. 6A). These data demonstrate that lack of IgM within the retina leads to significant long-term reactive gliosis in multiple glia types.

As reactive gliosis can be associated with outer BRB degeneration [67, 68], we examined the RPE, which is an integral component of the outer barrier. The RPE is a monolayer of pigmented cells found in the retina, which play a critical role in retinal homeostasis, including maintenance of the BRB and the immune-regulatory environment [36]. Previously, it was shown that the RPE becomes multinucleated during the aging process in mice, which is attributed to failed cytokinesis in response to age-related oxidative stress resulting from changes in retinal architecture [69]. Herein, we examined the nucleation state of the RPE in WT and μ s^{-/-} mice using H&E staining. With H&E staining, the RPE showed no differences between young WT and μ s^{-/-} mice. Interestingly, the proportion of cells with single nuclei versus multinucleate RPE cells was significantly increased in aged μ s^{-/-} mice as compared to aged WT mice (Fig. 7A-C; white arrows indicate binucleated RPE cells). In aged WT mice, the majority of RPE cells from the retina (peripheral/equatorial regions) were mononucleate ($97.133\% \pm 0.416$), while aged μ s^{-/-} mice showed a significant decrease in mononucleate RPE

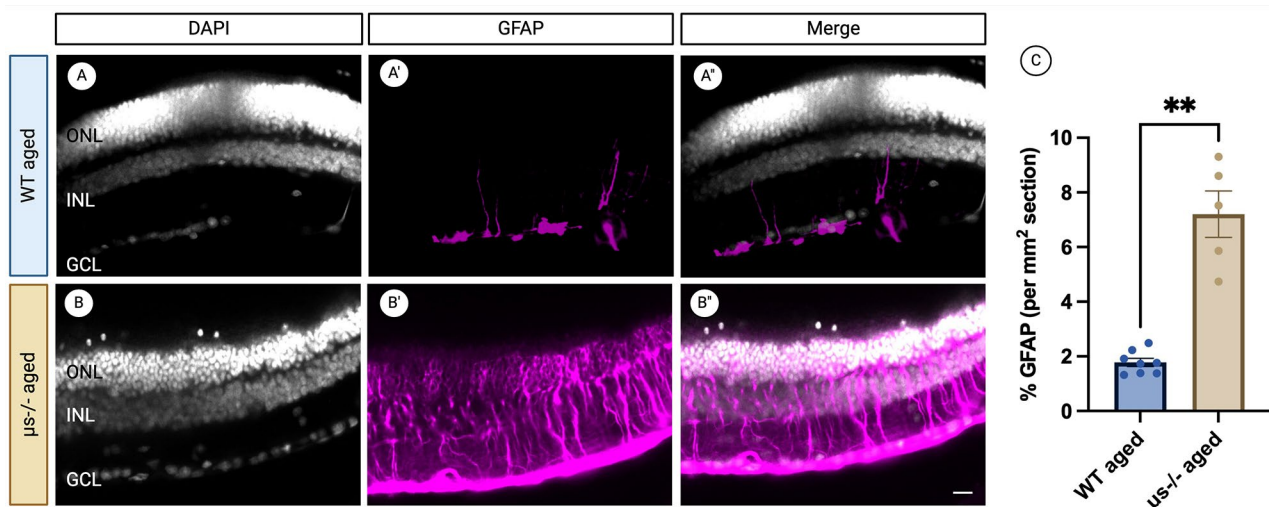


Fig. 6 Increased reactive gliosis in aged mice lacking IgM. Cross sections of aged WT (A-A') and aged μ s^{-/-} (B-B') were examined for active Müller glia. Sections were stained for GFAP (magenta) and DAPI (gray) for visualization of MG. Total percent GFAP measured (C) as an average of 10 sections per animal, with two independent experiments performed. Each point represents the average of 1 animal. Total animals used: WT aged $n = 8$, μ s^{-/-} aged $n = 5$. Statistics used: Mann Whitney. * $p < 0.05$, ** $p < 0.01$. Scale bar: 50 μ m

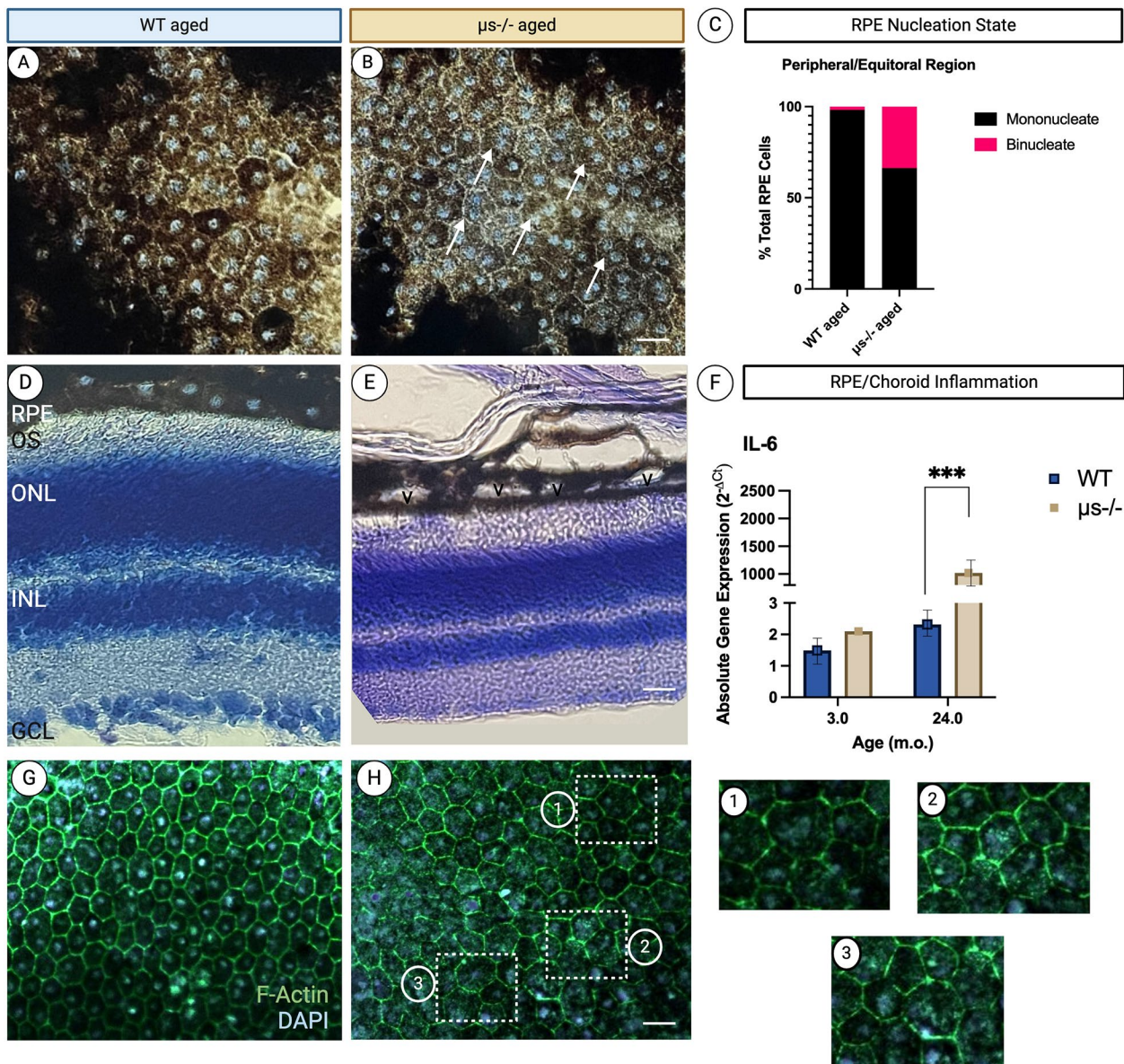


Fig. 7 Lack of IgM is associated with RPE stress and barrier dysfunction in aged mice. Retinas were dissected out of aged (24mo) WT and μ S-/- mice; one eye was used for H&E and one eye was used for RNA extraction. **(A)** Representative image of H&E RPE flat mount from an aged WT mouse compared to **(B)** representative image of that from an aged μ S-/- mouse. **(C)** RPE cells from the peripheral/equatorial region of the retina were counted and averaged to be either (1) mononucleate (only 1 nucleus/cell) or (2) multinucleate (≥ 2 nuclei/cell). **(D)** H&E retinal sections from an aged WT mouse compared to **(E)** the aged μ S-/- retina shows signs of retinal degeneration in the neural retina and RPE layer including extensive vacuolation (labeled as “V” in **(E)**). **(F)** RNA was isolated from the RPE of both young and aged retinas, and qPCR was performed to determine expression level of the inflammatory cytokine IL-6. **(G&H)** Cytoskeleton changes are seen in RPE from aged μ S-/- mice **(H)** as compared to aged WT mice **(G)** through examination of F-actin. Both aging WT and μ S-/- RPE show typical age-related changes with increase in RPE size and changes in regular polygonal geometry and shape. However, μ S-/- aged mice **(H)** show further evidence of RPE stress and barrier dysfunction such irregular morphology (1), the presence to intracellular stress fibers, with fraying and thickening (2), and fragmentation of the RPE cytoskeleton (3). Results based on three independent experiments. Statistics used: unpaired, two-tailed Mann-Whitney U test. $***p < 0.001$. Animals used: Young WT $n = 10$; Young μ S-/- $n = 12$; Aged WT $n = 7$; Aged μ S-/- $n = 5$. Scale bar = 50 μ m

cells ($66.233\% \pm 2.558$; $p = 0.001$). This significant increase in polynucleated RPE indicates that lack of IgM leads to increased RPE stress. Upon examination of retinal H&E cross sections, the μ S-/- retina (Fig. 7E) demonstrated characteristic retinal degeneration associated with a lack

of IgM, as compared to the WT retina (Fig. 7D). When examining the RPE layer, it was evident that the WT RPE is a tightly associated monolayer. However, μ S-/- mice exhibited significant degeneration of the RPE layer, including extensive vacuolation (Fig. 7E, “V”).

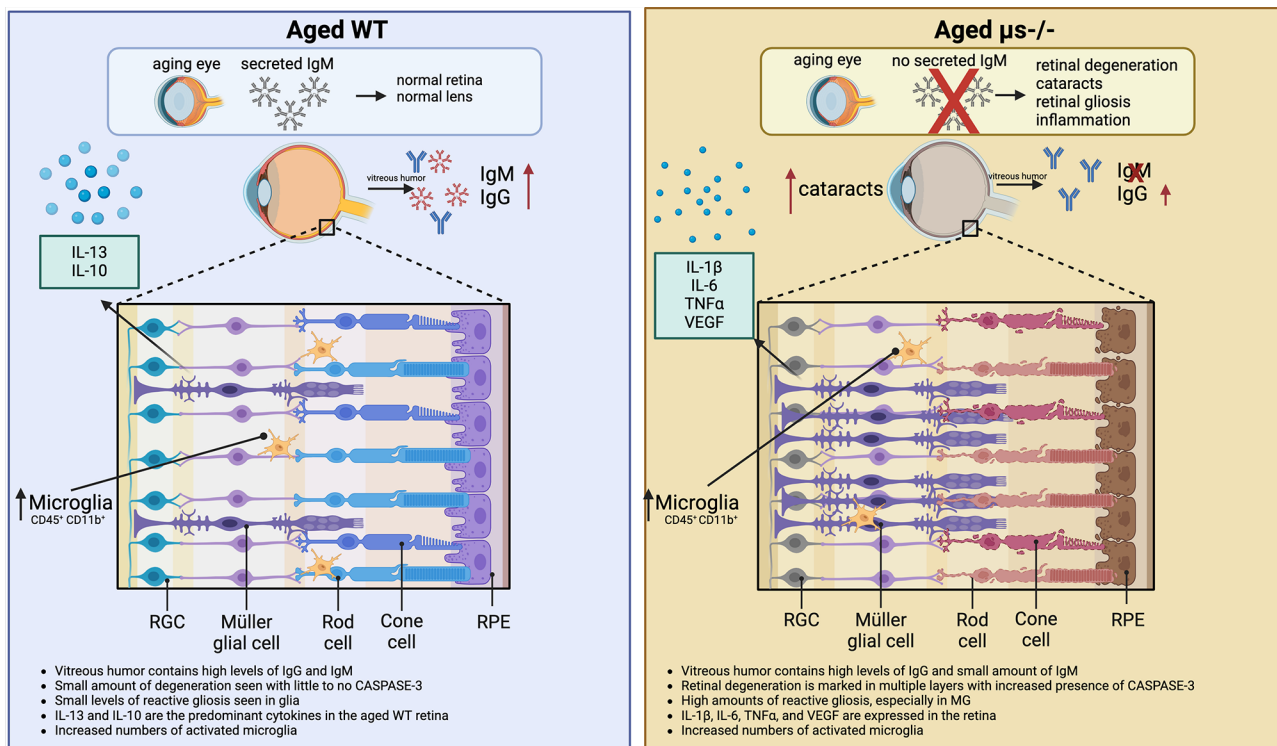


Fig. 8 Summary of findings and proposed model identifying a role of secreted IgM in retinal maintenance during aging. This study highlights the contribution of secreted IgM in the maintenance of retinal health during aging. During normal aging, we observed a minor loss of retinal neurons, accompanied by a slight increase in activated microglia, which appear to be effectively modulated by resident Müller glia. In $\mu s^{-/-}$ mice lacking secreted IgM, we noted significant neurodegeneration during aging, along with an increase in apoptotic cells. These observations suggest a potential role for IgM in facilitating the clearance of apoptotic debris from the retina, consistent with its established function in immune regulation elsewhere in the body. Additionally, we observed alterations in the retinal cytokine profile in the absence of secreted IgM, characterized by elevated levels of pro-inflammatory cytokines and a marked reduction in anti-inflammatory cytokines, compared to the relatively balanced profile observed in aging WT mice. This pro-inflammatory shift in the absence of IgM was accompanied by significant reactive gliosis in some resident Müller glia. Together, these findings indicate that secreted IgM may contribute to retinal homeostasis during aging by modulating inflammatory responses and maintaining a supportive environment for neuronal health. Future studies will be necessary to further define the mechanisms underlying these observations and to explore the role of IgM in retinal health during advanced aging. Created in BioRender. Webster, S. (2024) BioRender.com/r68o468

We investigated the function of the BRB by examining IL-6 expression via RT-qPCR in isolated RPE tissue from both young and aged WT and $\mu s^{-/-}$ retinas. IL-6 signaling decreases barrier function and increases vascular leakage [70]. We found that in the absence of secreted IgM, there was a significant increase in IL-6 within the RPE of aged $\mu s^{-/-}$ compared with aged WT mice (Fig. 7F; $p = 0.001$). Additionally, we examined RPE morphology using actin staining (Fig. 7G and H). As seen with typical aging, both WT and $\mu s^{-/-}$ mice have increased irregular geometry and size, whereas the RPE seen in the young usually maintain a normal, uniform, polygonal patterning. However, unlike aged WT mice, aged $\mu s^{-/-}$ mice show further irregularities in their appearance, including irregular morphology (Fig. 7H, callout 1), the presence of intracellular stress fibers, with fraying and thickening (Fig. 7H, callout 2), and fragmentation of the RPE cytoskeleton (Fig. 7H, callout 3). This type of damage is also observed in other age-related retinopathies, such as age-related macular degeneration [71]. These results demonstrate

that the lack of IgM significantly changes the RPE layer with age; the RPE cells display signs of cellular stress, which results in BRB compromise and increased IL-6 expression in the RPE.

In addition to retinal degeneration, we observed other ocular consequences with a lack of secreted IgM, such as cataract formation. We found that opacity was lost in $\mu s^{-/-}$ lenses, along with a significant increase in cataract incidence (Supplemental Figure S6).

While our data suggest that the absence of secreted IgM directly alters the local retinal microenvironment by increasing inflammation and reactive gliosis, it is plausible that systemic changes resulting from IgM deficiency contribute indirectly to the enhanced neurodegeneration. For example, IgM can inhibit microvesicle-driven coagulation and thrombosis [72] and an increase in thrombosis has been shown to increase retinal degeneration [73]. Therefore, we hypothesized that lack of IgM could lead to increased thrombosis causing the observed increase in retinal degeneration in $\mu s^{-/-}$ mice. Evidence of blood

clotting can be measured by D-dimer in the serum. We evaluated the serum of young and aged WT and *us*^{-/-} mice for D-dimer. Our results showed that despite lack of circulating IgM, levels of D-dimer in the mouse did not change regardless of age (Supplemental Figure S7). Further studies are needed to elucidate the direct and/or indirect contributions of IgM to retinal degeneration.

Discussion

Ocular homeostasis for vision maintenance is an essential physiological process, as vision loss is a significant burden on individuals and the global healthcare system. Lymphocytes have been shown to play a role in the eye during ocular disease and inflammation; *in vitro* studies have shown B cell interaction with the retinal endothelium [61]. However, little is known about the role of B cells and the antibodies they produce in normal ocular homeostasis. Some evidence exists for lymphocytes providing a surveillance function in the CNS [74, 75]. Additionally, extrapolating from research in other CNS tissues, B cells may enter the retina to participate in physiological immune surveillance [61, 74]. In particular, B cells have been shown to reside within the CNS in limited numbers in young individuals, with increasing numbers observed during aging [76]. Furthermore, a monoclonal IgM, HlgM12, has been shown to bind neurons, support neurite extension, and override neurite outgrowth inhibition [77, 78]. A recent shift in our understanding of multiple sclerosis (MS) has demonstrated that antibody-dependent and antibody-independent mechanisms are thought to underlie B cell-mediated CNS injury in MS [79, 80]. These reports demonstrate a role for B cells and the Ig they produce in CNS tissue. Here, we present a novel finding that increased degeneration of the retina and loss of optical clarity in the lens were observed in the absence of secreted IgM, in conjunction with significant changes in retinal cytokines from an anti-inflammatory profile to a largely pro-inflammatory retinal environment. With these changes, a lack of IgM leads to significant reactive gliosis. These findings are intriguing in context to the well-known functions of the blood-retinal barrier (BRB); the RPE is a major component of the BRB, and it is hypothesized that as antibodies are poorly permeating, their bioavailability is limited under homeostatic conditions [81]. However, our findings suggest antibodies play an important role in aiding in the maintenance of retinal health, which adds to the current understanding of ocular maintenance.

Unexpectedly, we detected a small amount of IgM within the vitreous humor of aged in *us*^{-/-} mice. This seemingly paradoxical increase in IgM in the vitreous humor (VH) of *us*^{-/-} mice during aging must be contextualized within the broader framework of IgM availability and function. First, as demonstrated by our results,

serum IgM was not detected in young or aged *us*^{-/-} mice. These findings suggest that IgM in the vitreous humor originates from an alternative source. The limited IgM detected in the VH of *us*^{-/-} mice may be residual or sequestered within pathological contexts, potentially derived from dying B cells or extracellular vesicles. However, further studies are needed to clarify the role of these alternative IgM sources in the VH of *us*^{-/-} mice. This IgM, even if bioavailable, appears insufficient to counterbalance the inflammatory milieu and reactive gliosis observed in these mice. Consequently, the lack of functional IgM contributes to an environment permissive to increased inflammation and gliosis, exacerbating neurodegeneration, rather than mitigating it.

The lack of secreted IgM resulted in heightened reactive gliosis and inflammation, contributing to the worsening progression of retinal degeneration with age in the *us*^{-/-} mice as compared to WT counterparts. In the absence of the *rd8* allele, we found significant neural degeneration across all retinal layers in aged *us*^{-/-} mice due to increased apoptosis, as evidenced by the increased levels of activated caspase-3 and TUNEL-positive cells. Importantly, natural IgM binds to apoptotic cells, facilitating the recruitment of C1q, which enhances apoptotic cell clearance by phagocytes [54, 82]. Although IgM has not previously been shown to play a role in the retina, complement receptors are found on the RPE and microglia [83–85], and both cells can clear debris. The RPE are known to play a role in apoptotic clearance [86] while microglia have a clear role in phagocytosis through interaction with C1q [87]. Based on the data presented herein, it is possible that IgM aids the RPE in apoptotic clearance under homeostatic conditions, or interacts with microglia to clear typical cellular debris. Importantly, in the absence of IgM we observed increased cell death and a build-up of apoptotic cells, which was not observed in aged mice capable of IgM secretion. The role of IgM and complement receptors in the retina will be an interesting avenue for further inquiry. Although IgM may directly contribute to the maintenance of retinal health, it is also important to consider the potential systemic effects of IgM deficiency on the observed retinal degeneration. Selective IgM deficiency can be associated with autoimmune diseases [88–91], which could potentially contribute to retinal degeneration in advanced age through mechanisms that remain to be elucidated.

With enhanced retinal neurodegeneration in mice lacking IgM, we found a significant change in the retinal inflammatory profile as well as the resident glia. The absence of IgM reversed the cytokine profile from that of high IL-10 and IL-13 levels maintained during healthy aging (anti-inflammatory) to that of high IL-1 β , IL-6, TNF α , and VEGF (pro-inflammatory) levels. This marked switch in cytokine expression is associated with increased microglial

proliferation and reactivity. In the absence of IgM, microglia displayed a change in the transformation index (TI), developing an amoeboid shape with large cell bodies, indicative of microglia activation. Activated microglia are a primary marker of neurodegeneration [4, 6, 7, 63]. We found an increase in the MFI of CD86 on microglia in young μ s-/- compared to WT young retinas. This is interesting in the context of the microenvironment of the retina, which demonstrates a slight shift in cytokine profiles during the transition from early to older age. However, regardless of the presence or absence of IgM, increased activated microglia were observed in aged mice, which is consistent with literature [5, 9]. These data suggest that a lack of IgM does not influence the proliferation or migration of microglia to inflamed and damaged retinas with age. Nevertheless, there has been increasing evidence that microglia are activated on a spectrum that could accommodate the fluctuating degeneration rates of different retinal neuron subtypes [92]. However, the exact role and mechanism of how IgM influences the activation of microglia warrants further investigation.

We also observed significant reactive gliosis in both retinal astrocytes and Müller glia (MG) in the absence of IgM. GFAP expression was significantly increased in mice lacking IgM, especially aged mice. A high level of reactive gliosis is an indication of gliosis-based neurodegeneration [8]. Together, these data add to our understanding of the complex regulatory systems involved in retinal maintenance. Herein, we observed that in the absence of IgM apoptotic debris accumulates in the neural retina, there is a significant increase in pro-inflammatory cytokines, degeneration of the outer BRB, and significant gliosis, as well as enhanced retinal degeneration in aging mice (summarized in Fig. 8). This is the first study to demonstrate a role for IgM in the maintenance of retinal health into advanced age. Although it is still unknown whether this role of IgM is direct or indirect, continued research into the interplay between B cells, IgM, and the retina is necessary to better understand ocular diseases and potential treatments.

Supplementary Information

The online version contains supplementary material available at <https://doi.org/10.1186/s12979-025-00502-2>.

Supplementary Material 1

Acknowledgements

We thank the Flow Cytometry and Imaging Core at WMU Homer Stryker M.D. School of Medicine for the use of and assistance with both the flow cytometry and confocal microscopy work presented here. We thank the Swirski Lab for sharing detailed protocol for tissue digestion done in this work. We thank Jeffrey Young within the WMed Department of Biomedical Informatics for biostatistics assistance. Figures were generated with BioRender.com.

Author contributions

S.W. and N.H. conceptualized the manuscript. S.W., M.C., N.H., and P.J. all worked out the methodology for this research project. S.W., S.L., N.D., D.H., N.T.,

M.C., and N.H. all performed experiments and data analysis. S.W., S.L., N.D., and N.H. prepared all figures. S.W. wrote the main manuscript text and S.W., M.C., P.J., and N.H. edited the manuscript. All authors reviewed the manuscript.

Funding

Research reported in this publication was supported by the National Institute of Allergy and Infectious Disease (NIAID) of the National Institutes of Health (NIH) under award 1R01AI154539-01 (NEH), F32AI174673-01A1 (SEW), and supported by the National Institute on Aging (NIA) of the NIH under award R01AG084752 (NEH). The content is solely the responsibility of the authors and does not necessarily represent the official views of the NIH.

Data availability

No datasets were generated or analysed during the current study.

Declarations

Ethical approval

Mice were cared for and handled in accordance with the *Guide for the Care and Use of Laboratory Animals* (National Institutes of Health) and institutional guidelines. All animal studies were approved by the Institutional Animal Care and Use Committee at Western Michigan University Homer Stryker M.D. School of Medicine.

Consent for publication

Not applicable.

Competing interests

The authors declare no competing interests.

Received: 18 October 2024 / Accepted: 8 February 2025

Published online: 24 February 2025

References

1. NIA. Aging and Your Eyes. Natl. Institutes Heal. 2021.
2. London A, Benhar I, Schwartz M. The retina as a window to the brain—from eye research to CNS disorders. *Nat Rev Neurol* [Internet]. 2013;9:44–53. Available from: <https://doi.org/10.1038/nrneurol.2012.227>
3. Masland RH. The fundamental plan of the retina. *Nat Neurosci* [Internet]. 2001;4:877–86. Available from: <https://doi.org/10.1038/nn0901-877>
4. Zhou T, Huang Z, Sun X, Zhu X, Zhou L, Li M et al. Microglia Polarization with M1/M2 Phenotype Changes in rd1 Mouse Model of Retinal Degeneration [Internet]. *Front. Neuroanat.* 2017. Available from: <https://www.frontiersin.org/articles/https://doi.org/10.3389/fnana.2017.00077>
5. Guo S, Wang H, Yin Y. Microglia Polarization From M1 to M2 in Neurodegenerative Diseases [Internet]. *Front. Aging Neurosci.* 2022. Available from: <https://www.frontiersin.org/articles/https://doi.org/10.3389/fnagi.2022.815347>
6. Colonna M, Butovsky O. Microglia Function in the Central Nervous System During Health and Neurodegeneration. *Annu Rev Immunol* [Internet]. *Annual Reviews*; 2017;35:441–68. Available from: <https://doi.org/10.1146/annurev-immunol-051116-052358>
7. Tang Y, Le W. Differential Roles of M1 and M2 Microglia in Neurodegenerative Diseases. *Mol Neurobiol* [Internet]. 2016;53:1181–94. Available from: <https://doi.org/10.1007/s12035-014-9070-5>
8. Fernández-Sánchez L, Lax P, Campello L, Pinilla I, Cuenca N. Astrocytes and Müller Cell Alterations During Retinal Degeneration in a Transgenic Rat Model of Retinitis Pigmentosa [Internet]. *Front. Cell. Neurosci.* 2015. Available from: <https://www.frontiersin.org/articles/https://doi.org/10.3389/fncel.2015.00484>
9. Chen M, Luo C, Zhao J, Devarajan G, Xu H. Immune regulation in the aging retina. *Prog Retin Eye Res* [Internet]. 2019;69:159–72. Available from: <https://www.sciencedirect.com/science/article/pii/S1350946218300442>
10. Chan C, Rubenstein JL, Coupland SE, Davis JL, Harbour JW, Johnston PB et al. Primary Vitreoretinal Lymphoma: A Report from an International Primary Central Nervous System Lymphoma Collaborative Group Symposium. *Oncologist* [Internet]. 2011;16:1589–99. Available from: <https://doi.org/10.1634/theoncologist.2011-0210>
11. Fekkar A, Bodaghi B, Touafek F, Le Hoang P, Mazier D, Paris L. Comparison of Immunoblotting, Calculation of the Goldmann-Witmer Coefficient, and

- Real-Time PCR Using Aqueous Humor Samples for Diagnosis of Ocular Toxoplasmosis. *J Clin Microbiol* [Internet]. American Society for Microbiology; 2008;46:1965–7. Available from: <https://doi.org/10.1128/JCM.01900-07>
12. Palestine AG, Nussenblatt RB, Chan C-C, Hooks JJ, Friedman L, Kuwabara T. Histopathology of the Subretinal Fibrosis and Uveitis Syndrome. *Ophthalmology* [Internet]. 1985;92:838–44. Available from: <https://www.sciencedirect.com/science/article/pii/S0161642085339696>
 13. Chan C-C, Palestine AG, Kuwabara T, Nussenblatt RB. Immunopathologic Study of Vogt-Koyanagi-Harada Syndrome. *Am J Ophthalmol* [Internet]. 1988;105:607–11. Available from: <https://www.sciencedirect.com/science/article/pii/S0002939488900529>
 14. Walport MJ, Complement. First of Two Parts. *N Engl J Med* [Internet]. Massachusetts Medical Society; 2001;344:1058–66. Available from: <https://doi.org/10.1056/NEJM200104053441406>
 15. Walport MJ, Complement. Second of Two Parts. *N Engl J Med* [Internet]. Massachusetts Medical Society; 2001;344:1140–4. Available from: <https://doi.org/10.1056/NEJM200104123441506>
 16. LeBien TW, Tedder TF. B lymphocytes: how they develop and function. *Blood* United States. 2008;112:1570–80.
 17. Hardy RR. B-1 B Cell Development. *J Immunol* [Internet]. 2006;177:2749 LP – 2754. Available from: <http://www.jimmunol.org/content/177/5/2749.abstract>
 18. Holodick NE, Rodríguez-Zhurbenko N, Hernández AM. Defining natural antibodies. *Front Immunol*. 2017;8:2–9.
 19. Haas KM, Poe JC, Steeber DA, Tedder TF. B-1a and B-1b cells exhibit distinct developmental requirements and have unique functional roles in innate and adaptive immunity to *S. pneumoniae*. *Immunity*. 2005;23:7–18.
 20. Boes M, Prodeus AP, Schmidt T, Carroll MC, Chen J. A critical role of natural immunoglobulin M in immediate defense against systemic bacterial infection. *J Exp Med* [Internet]. The Rockefeller University Press; 1998;188:2381–6. Available from: <https://pubmed.ncbi.nlm.nih.gov/9858525>
 21. Alugupalli KR, Gerstein RM, Chen J, Szomolanyi-Tsuda E, Woodland RT, Leong JM. The Resolution of Relapsing Fever Borreliosis Requires IgM and Is Concurrent with Expansion of B1b Lymphocytes. *J Immunol* [Internet]. 2003;170:3819 LP – 3827. Available from: <http://www.jimmunol.org/content/170/7/3819.abstract>
 22. Baumgarth N, Herman OC, Jager G, Brown L, Herzenberg LA, Herzenberg LA. Innate and acquired humoral immunities to influenza virus are mediated by distinct arms of the immune system. *Proc Natl Acad Sci* [Internet]. Proceedings of the National Academy of Sciences; 1999;96:2250–5. Available from: <https://doi.org/10.1073/pnas.96.5.2250>
 23. Ochsenbein AF, Fehr T, Lutz C, Suter M, Brombacher F, Hengartner H et al. Control of Early Viral and Bacterial Distribution and Disease by Natural Antibodies. *Science* (80-) [Internet]. American Association for the Advancement of Science; 1999;286:2156–9. Available from: <https://doi.org/10.1126/science.286.5447.2156>
 24. Subramaniam KS, Datta K, Quintero E, Manix C, Marks MS, Pirofski L. The Absence of Serum IgM Enhances the Susceptibility of Mice to Pulmonary Challenge with *Cryptococcus neoformans* *J Immunol* [Internet]. 2010;184:5755 LP – 5767. Available from: <http://www.jimmunol.org/content/184/10/5755.abstract>
 25. Rapaka RR, Ricks DM, Alcorn JF, Chen K, Khader SA, Zheng M et al. Conserved natural IgM antibodies mediate innate and adaptive immunity against the opportunistic fungus *Pneumocystis murina*. *J Exp Med* [Internet]. 2010/12/13. The Rockefeller University Press; 2010;207:2907–19. Available from: <https://pubmed.ncbi.nlm.nih.gov/21149550>
 26. Grönwall C, Vas J, Silverman G. Protective Roles of Natural IgM Antibodies [Internet]. *Front Immunol*. 2012. Available from: <https://www.frontiersin.org/article/https://doi.org/10.3389/fimmu.2012.00066>
 27. Tsiantoulas D, Kiss M, Bartolini-Gritti B, Bergthaler A, Mallat Z, Jumaa H, et al. Secreted IgM deficiency leads to increased BCR signaling that results in abnormal splenic B cell development. *Sci Rep Springer US*. 2017;7:1–9.
 28. Zhang M, Alicot EM, Chiu I, Li J, Verna N, Vorup-Jensen T et al. Identification of the target self-antigens in reperfusion injury. *J Exp Med* [Internet]. 2006/01/03. The Rockefeller University Press; 2006;203:141–52. Available from: <https://pubmed.ncbi.nlm.nih.gov/16390934>
 29. Binder CJ, Silverman GJ. Natural antibodies and the autoimmunity of atherosclerosis. *Springer Semin Immunopathol* [Internet]. 2005;26:385–404. Available from: <https://doi.org/10.1007/s00281-004-0185-z>
 30. Binder CJ, Shaw PX, Chang M-K, Boullier A, Hartvigsen K, Hörkö S, et al. The role of natural antibodies in atherogenesis. *J Lipid Res United States*. 2005;46:1353–63.
 31. Meek B, Speijer D, De Jong PTVM, De Smet MD, Peek R. The ocular humoral immune response in health and disease. *Prog Retin Eye Res*. 2003;22:391–415.
 32. Tsuji N, Rothstein TL, Holodick NE. Antigen receptor specificity and cell location influence the diversification and selection of the B-1a Cell Pool with Age. *J Immunol*. 2020;205:741–59.
 33. Webster SE, Ryali B, Clemente MJ, Tsuji N, Holodick NE. Sex influences age-related changes in natural antibodies and CD5+ B-1 cells. *J Immunol*. 2022;208:1–17.
 34. Webster SE, Tsuji NL, Clemente MJ, Holodick NE. Age-related changes in antigen-specific natural antibodies are influenced by sex [Internet]. *Front Immunol*. 2023. Available from: <https://www.frontiersin.org/articles/https://doi.org/10.3389/fimmu.2022.1047297>
 35. Webster SE, Sklar NC, Spitsbergen JB, Stanchfield ML, Webster MK, Linn DM et al. Stimulation of $\alpha 7$ nAChR leads to regeneration of damaged neurons in adult mammalian retinal disease models. *Exp Eye Res* [Internet]. 2021;210:108717. Available from: <https://www.sciencedirect.com/science/article/pii/S0014483521002839>
 36. Webster SE, Spitsbergen JB, Linn DM, Webster MK, Otteson D, Cooley-Themm C et al. Transcriptome Changes in Retinal Pigment Epithelium Post-PNU-282987 Treatment Associated with Adult Retinal Neurogenesis in Mice. *J Mol Neurosci* [Internet]. 2022;72:1990–2010. Available from: <https://doi.org/10.1007/s12031-022-02049-z>
 37. Shang P, Stepicheva NA, Hose S, Zigler JSJ, Sinha D. Primary cell cultures from the mouse retinal pigment epithelium. *J Vis Exp United States*; 2018.
 38. Pang J, Thomas N, Tsuchiya D, Parmely T, Yan D, Xie T et al. Step-by-step preparation of mouse eye sections for routine histology, immunofluorescence, and RNA in situ hybridization multiplexing. *STAR Protoc* [Internet]. 2021;2:100879. Available from: <https://www.sciencedirect.com/science/article/pii/S2666166721005852>
 39. Weber GF, Chousterman BG, Hilgendorf I, Robbins CS, Theurl I, Gerhardt LMS, et al. Pleural innate response activator B cells protect against pneumonia via a GM-CSF-IgM axis. *J Exp Med*. 2014;211:1243–56.
 40. Billing RJ, Safani M, Peterson P. Isolation and characterization of human B cell alloantigens. *J Immunol United States*. 1976;117:1589–93.
 41. Cambier JC, Vitetta ES, Kettman JR, Wetzel GM, Uhr JW. B-cell tolerance. III. Effect of papain-mediated cleavage of cell surface IgD on tolerance susceptibility of murine B cells. *J Exp Med United States*. 1977;146:107–17.
 42. Dwyer DF, Woodruff MC, Carroll MC, Austen KF, Gurish MF. B cells regulate CD4+ T cell responses to papain following B cell receptor-independent papain uptake. *J Immunol United States*. 2014;193:529–39.
 43. Dosch HM, Kwong S, Tsui F, Zimmerman B, Gelfand EW. Role of surface IgM and IgD in the functional differentiation of human B lymphocytes: effect of papain treatment. *J Immunol United States*. 1979;123:557–60.
 44. Fortmann SD, Lorenc VE, Shen J, Hackett SF, Campochiaro PA. Mousetap, a Novel Technique to Collect Uncontaminated Vitreous or Aqueous and Expand Usefulness of Mouse Models. *Sci Rep* [Internet]. 2018;8:6371. Available from: <https://doi.org/10.1038/s41598-018-24197-2>
 45. Church KA, Rodriguez D, Vanegas D, Gutierrez IL, Cardona SM, Madrigal JLM, et al. Models of microglia depletion and replenishment elicit protective effects to alleviate vascular and neuronal damage in the diabetic murine retina. *J Neuroinflammation Engl*. 2022;19:300.
 46. Sarker B, Cardona SM, Church KA, Vanegas D, Velazquez P, Rorex C, et al. Defibrinogenation ameliorates retinal microgliosis and inflammation in a CX3CR1-Independent manner. *ASN Neuro United States*. 2022;14:17590914221131446.
 47. Allansmith MR, Whitney CR, McClellan BH, Newman LP. Immunoglobulins in the Human Eye: Location, Type, and Amount. *Arch Ophthalmol* [Internet]. 1973;89:36–45. Available from: <https://doi.org/10.1001/archoph.1973.01000040038010>
 48. Sen DK, Sarin GS, Saha K. Immunoglobulins in human aqueous humour. *Br J Ophthalmol*. 1977;61:216–7.
 49. Rose GE, Billington BM, Chignell AH. Immunoglobulins in paired specimens of vitreous and subretinal fluids from patients with rhegmatogenous retinal detachment. *Br J Ophthalmol Engl*. 1990;74:160–2.
 50. Murueta-Goyena A, Del Pino R, Acera M, Teixeira-Portas S, Romero D, Ayala U et al. Retinal thickness as a biomarker of cognitive impairment in manifest Huntington's disease. *J Neurol* [Internet]. 2023;270:3821–9. Available from: <https://doi.org/10.1007/s00415-023-11720-3>
 51. Alamouti B, Funk J. Retinal thickness decreases with age: an OCT study. *Br J Ophthalmol* [Internet]. 2003;87:899 LP – 901. Available from: <http://bjo.bmj.com/content/87/7/899.abstract>

52. Ogden CA, Kowalewski R, Peng Y, Montenegro V, Elkon KB. IGM is required for efficient complement mediated phagocytosis of apoptotic cells in vivo. *Autoimmunity* [Internet]. Taylor & Francis; 2005;38:259–64. Available from: <https://doi.org/10.1080/08916930500124452>
53. Quartier P, Potter PK, Ehrenstein MR, Walport MJ, Botto M. Predominant role of IgM-dependent activation of the classical pathway in the clearance of dying cells by murine bone marrow-derived macrophages in vitro. *Eur J Immunol* [Internet]. John Wiley & Sons, Ltd; 2005;35:252–60. Available from: <https://doi.org/10.1002/eji.200425497>
54. Chen Y, Park Y-B, Patel E, Silverman GJ. IgM Antibodies to Apoptosis-Associated Determinants Recruit C1q and Enhance Dendritic Cell Phagocytosis of Apoptotic Cells1. *J Immunol* [Internet]. 2009;182:6031–43. Available from: <https://doi.org/10.4049/jimmunol.0804191>
55. Mehalow AK, Kameya S, Smith RS, Hawes NL, Denegre JM, Young JA, et al. CRB1 is essential for external limiting membrane integrity and photoreceptor morphogenesis in the mammalian retina. *Hum Mol Genet*. 2003;12:2179–89.
56. Mattapallil MJ, Wawrousek EF, Chan C-C, Zhao H, Roychoudhury J, Ferguson TA et al. The Rd8 Mutation of the Crb1 Gene Is Present in Vendor Lines of C57BL/6 N Mice and Embryonic Stem Cells, and Confounds Ocular Induced Mutant Phenotypes. *Invest Ophthalmol Vis Sci* [Internet]. 2012;53:2921–7. Available from: <https://doi.org/10.1167/iov.12-9662>
57. Notley CA, Brown MA, Wright GP, Ehrenstein MR. Natural IgM is required for suppression of inflammatory arthritis by apoptotic cells. *J Immunol United States*. 2011;186:4967–72.
58. Grönwall C, Silverman GJ. Natural IgM: beneficial autoantibodies for the control of inflammatory and autoimmune disease. *J Clin Immunol Neth*. 2014;34(Suppl 1):S12–21.
59. Ghasemi H. Roles of IL-6 in Ocular Inflammation: A Review. *Ocul Immunol Inflamm* [Internet]. Taylor & Francis; 2018;26:37–50. Available from: <https://doi.org/10.1080/09273948.2016.1277247>
60. Burmeister AR, Marriott I. The Interleukin-10 Family of Cytokines and Their Role in the CNS [Internet]. *Front. Cell. Neurosci*. 2018. Available from: <https://www.frontiersin.org/articles/https://doi.org/10.3389/fncel.2018.00458>
61. Bharadwaj AS, Stempel AJ, Olivas A, Franzese SE, Ashander LM, Ma Y et al. Molecular Signals Involved in Human B Cell Migration into the Retina: In Vitro Investigation of ICAM-1, VCAM-1, and CXCL13. *Ocul Immunol Inflamm* [Internet]. Taylor & Francis; 2017;25:811–9. Available from: <https://doi.org/10.1080/09273948.2016.1180401>
62. Karaahmet B, Le L, Mendes MS, Majewska AK, O'Banion MK. Repopulated microglia induce expression of Cxcl13 with differential changes in Tau phosphorylation but do not impact amyloid pathology. *J Neuroinflammation* [Internet]. 2022;19:173. Available from: <https://doi.org/10.1186/s12974-022-02532-9>
63. Prinz M, Priller J. Microglia and brain macrophages in the molecular age: from origin to neuropsychiatric disease. *Nat Rev Neurosci* [Internet]. 2014;15:300–12. Available from: <https://doi.org/10.1038/nrn3722>
64. Gerganova G, Riddell A, Miller AA. CNS border-associated macrophages in the homeostatic and ischaemic brain. *Pharmacol Ther* [Internet]. 2022;240:108220. Available from: <https://www.sciencedirect.com/science/article/pii/S0163725822001140>
65. Sun R, Jiang H. Border-associated macrophages in the central nervous system. *J Neuroinflammation* [Internet]. 2024;21:67. Available from: <https://doi.org/10.1186/s12974-024-03059-x>
66. Zhang Y, Park YS, Kim I-BA. Distinct Microglial Cell Population expressing both CD86 and CD206 constitutes a Dominant type and executes phagocytosis in two mouse models of Retinal Degeneration. *Int J Mol Sci Switz*; 2023;24.
67. Napoli D, Biagioni M, Billeri F, Di Marco B, Orsini N, Novelli E et al. Retinal pigment epithelium remodeling in mouse models of Retinitis Pigmentosa. *Int J Mol Sci Switz*; 2021;22.
68. Martínez-Gil N, Maneu V, Kutsyr O, Fernández-Sánchez L, Sánchez-Sáez X, Sánchez-Castillo C et al. Cellular and molecular alterations in neurons and glial cells in inherited retinal degeneration. *Front Neuroanat* [Internet]. 2022;16. Available from: <https://www.frontiersin.org/journals/neuroanatomy/articles/https://doi.org/10.3389/fnana.2022.984052>
69. Chen M, Rajapakse D, Fraczek M, Luo C, Forrester JV, Xu H. Retinal pigment epithelial cell multinucleation in the aging eye – a mechanism to repair damage and maintain homeostasis. *Aging Cell* [Internet]. John Wiley & Sons, Ltd; 2016;15:436–45. Available from: <https://doi.org/10.1111/ace.12447>
70. Sharma S. Interleukin-6 Trans-signaling: A Pathway With Therapeutic Potential for Diabetic Retinopathy [Internet]. *Front. Physiol*. 2021. Available from: <https://www.frontiersin.org/articles/https://doi.org/10.3389/fphys.2021.689429>
71. Tarau I-S, Berlin A, Curcio CA, Ach T. The Cytoskeleton of the retinal pigment epithelium: from normal aging to age-related Macular Degeneration. *Int J Mol Sci*. 2019.
72. Obermayer G, Afonyushkin T, Göderle L, Puhm F, Schrottmaier W, Taqi S et al. Natural IgM antibodies inhibit microvesicle-driven coagulation and thrombolysis. *Blood* [Internet]. 2021;137:1406–15. Available from: <https://doi.org/10.1182/blood.2020007155>
73. Rehak M, Wiedemann P. Retinal vein thrombosis: pathogenesis and management. *J Thromb Haemost Engl*. 2010;8:1886–94.
74. Loeffler C, Dietz K, Schleich A, Schlasz H, Stoll M, Meyermann R et al. Immune surveillance of the normal human CNS takes place in dependence of the locoregional blood–brain barrier configuration and is mainly performed by CD3+/CD8+ lymphocytes. *Neuropathology* [Internet]. John Wiley & Sons, Ltd; 2011;31:230–8. Available from: <https://doi.org/10.1111/j.1440-1789.2010.01167.x>
75. Ousman SS, Kubes P. Immune surveillance in the central nervous system. *Nat Neurosci* [Internet]. 2012;15:1096–101. Available from: <https://doi.org/10.1038/nn.3161>
76. Jain RW, Yong VW. B cells in central nervous system disease: diversity, locations and pathophysiology. *Nat Rev Immunol* [Internet]. 2022;22:513–24. Available from: <https://doi.org/10.1038/s41577-021-00652-6>
77. Wootla B, Denic A, Warrington AE, Rodriguez M. A monoclonal natural human IgM protects axons in the absence of remyelination. *J Neuroinflammation* [Internet]. 2016;13:94. Available from: <https://doi.org/10.1186/s12974-016-0561-3>
78. Xu X, Ng SM, Hassouna E, Warrington A, Oh S-H, Rodriguez M. Human-derived natural antibodies: biomarkers and potential therapeutics. *Future Neurol* [Internet]. Future Medicine; 2015;10:25–39. Available from: <https://doi.org/10.2217/fnl.14.62>
79. Comi G, Bar-Or A, Lassmann H, Uccelli A, Hartung H-P, Montalban X et al. Role of B Cells in Multiple Sclerosis and Related Disorders. *Ann Neurol* [Internet]. John Wiley & Sons, Ltd; 2021;89:13–23. Available from: <https://doi.org/10.1002/ana.25927>
80. de Séze J, Maillart E, Gueguen A, Laplaud DA, Michel L, Thouvenot E et al. Anti-CD20 therapies in multiple sclerosis: From pathology to the clinic [Internet]. *Front. Immunol*. 2023. Available from: <https://www.frontiersin.org/article/https://doi.org/10.3389/fimmu.2023.1004795>
81. St-Amour I, Paré I, Alata W, Coulombe K, Ringuette-Goulet C, Drouin-Ouellet J. Brain Bioavailability of Human Intravenous Immunoglobulin and its Transport through the Murine Blood–Brain Barrier. *J Cereb Blood Flow Metab* [Internet]. SAGE Publications, Ltd STM et al. 2013;33:1983–92. Available from: <https://doi.org/10.1038/jcbfm.2013.160>
82. Elkon KB, Silverman GJ. Naturally Occurring Autoantibodies to Apoptotic Cells BT - Naturally Occurring Antibodies (NAbs). In: Lutz HU, editor. New York, NY: Springer New York; 2012. pp. 14–26. Available from: https://doi.org/10.1007/978-1-4614-3461-0_2
83. Luo C, Zhao J, Madden A, Chen M, Xu H. Complement expression in retinal pigment epithelial cells is modulated by activated macrophages. *Exp Eye Res Engl*. 2013;112:93–101.
84. Schäfer N, Wolf HN, Enzbrenner A, Schikora J, Reichenthaler M, Enzmann V, et al. Properdin modulates complement component production in stressed human primary retinal pigment epithelium cells. Basel, Switzerland: Antioxidants; Switzerland; 2020. p. 9.
85. Chen Y, Chu JM, Chang RC, Wong GT. The Complement System in the Central Nervous System: From Neurodevelopment to Neurodegeneration. *Biomolecules*. 2022.
86. Yang S, Zhou J, Li D. Functions and diseases of the retinal pigment epithelium. *Front Pharmacol Switz*. 2021;12:727870.
87. Scott-Hewitt N, Mahoney M, Huang Y, Korte N, Yvanka de Soysa T, Wilton DK et al. Microglial-derived C1q integrates into neuronal ribonucleoprotein complexes and impacts protein homeostasis in the aging brain. *Cell* [Internet]. Elsevier; 2024;187:4193–4212.e24. Available from: <https://doi.org/10.1016/j.cell.2024.05.058>
88. Nguyen TTT, Elsner RA, Baumgarth N. Natural IgM Prevents Autoimmunity by Enforcing B Cell Central Tolerance Induction. *J Immunol* [Internet]. 2015;194:1489 LP – 1502. Available from: <http://www.jimmunol.org/content/194/4/1489.abstract>
89. Gupta S, Gupta A. Selective IgM Deficiency—An Underestimated Primary Immunodeficiency. *Front Immunol Switz*. 2017;8:1056.
90. Shoughy SS, Tabbara KF. Ocular findings in systemic lupus erythematosus. *Saudi J Ophthalmol off J Saudi Ophthalmol Soc India*. 2016;30:117–21.

91. Saidha S, Syc SB, Ibrahim MA, Eckstein C, Warner CV, Farrell SK, et al. Primary retinal pathology in multiple sclerosis as detected by optical coherence tomography. *Brain Engl.* 2011;134:518–33.
92. Knudsen NH, Lee C-H, Identity Crisis. CD301b⁺ Mononuclear Phagocytes Blur the M1-M2 Macrophage Line. *Immunity* [Internet]. Elsevier; 2016;45:461–3. Available from: <https://doi.org/10.1016/j.immuni.2016.09.004>

Publisher's note

Springer Nature remains neutral with regard to jurisdictional claims in published maps and institutional affiliations.